
A FOUNDATION MODEL FOR ELECTRODERMAL ACTIVITY DATA

Leonardo Alchieri

Università della Svizzera Italiana (USI)
Via la Santa 1
6962 Lugano, Switzerland
leonardo.alchieri@usi.ch

Matteo Garzon

Università della Svizzera Italiana (USI)
Via la Santa 1
6962 Lugano, Switzerland

Lidia Alecci

Università della Svizzera Italiana (USI)
Via la Santa 1
6962 Lugano, Switzerland

Francesco Bombassei De Bona

Università della Svizzera Italiana (USI)
Via la Santa 1
6962 Lugano, Switzerland

Martin Gjoreski

Università della Svizzera Italiana (USI)
Via la Santa 1
6962 Lugano, Switzerland

Giovanni De Felice

Università della Svizzera Italiana (USI)
Via la Santa 1
6962 Lugano, Switzerland

Silvia Santini

Università della Svizzera Italiana (USI)
Via la Santa 1
6962 Lugano, Switzerland

March 19, 2026

Abstract

Foundation models have recently extended beyond natural language and vision to timeseries domains, including physiological signals. However, progress in electrodermal activity (EDA) modeling is hindered by the absence of largescale, curated, and openly accessible datasets. EDA reflects sympathetic nervous system activity and is widely used to infer cognitive load, stress, and engagement. Yet very few wearable devices provide continuous, unobtrusive sensing, and the only largescale archive to date is proprietary. To address this gap, we compile EDAMAME, a collection of EDA traces from 24 public datasets, comprising more than 25,000 hours from 634 users. Using this resource, we train UME, the first dedicated foundation model for EDA. In eight out of ten scenarios, UME outperforms baselines and matches generalist timeseries foundation models while using 20× fewer computational resources. Our findings, however, also highlight the intrinsic challenges of EDA modeling, motivating further research to unlock its full potential. All datasets, model weights, and code are released to support further research.

1 Introduction

Thanks to their ability to learn general patterns from broad, diverse data and to adapt them to a wide range of downstream tasks, foundation models have attracted attention beyond their traditional applications in natural language processing and computer vision. In particular, generalist foundation models for *time series*, like Mantis [35] or Chronos [8, 9], have been proposed recently. Trained on cross-domain dataset

collections, these models achieve remarkable performance on a diverse range of downstream tasks. Emerging foundation models for *physiological time series* data – e.g., for photoplethysmogram (PPG) [1, 72, 81, 32, 62], electrocardiogram (ECG) [1, 66, 59], and electroencephalogram (EEG) data [84] – show compelling performance, too. Yet their training remains constrained by the absence of largescale, curated, and open datasets for physiological signals. As highlighted by Abbaspourazad et al. [1] with respect to time series data in the medical domain, “*datasets are usually small in comparison to other domains, which is an obstacle for developing neural network models for biosignals*”.

This paucity of data is particularly acute for electrodermal activity (EDA) signals. EDA refers to changes in the skins electrical conductance caused by variations in sweat gland activity, which is itself regulated by the sympathetic branch of the autonomic nervous system. Alongside more commonly used physiological signals, EDA has numerous applications in personal informatics systems. Specifically, because EDA increases with physiological arousal, it is commonly used to assess cognitive load [52, 79], stress [39, 73], and engagement [36, 38, 19]. Yet EDA sensors are not (yet) commonplace on wearable devices and only few (such as, e.g., the Empatica E4 wristband) feature the unobtrusive, continuous measurement modality necessary to collect longitudinal traces of EDA in real-world settings. The only large-scale archive of EDA data is a proprietary dataset collected using the Fitbit Sense 2 [65]. This lack of (open) data has, to date, hampered the development of foundation models for EDA.

To cope with this challenge, we first constructed a large-scale archive of EDA data that integrates records from 24 different publicly available datasets and a total of more than 25’000 hours of data of 634 different users. We curated this collection of datasets, to which we refer to as EDAMAME (**EDA** Multi-dataset **A**rchive for **M**odel training and **E**valuation), to train a foundation model for EDA data. The model, called UME (fo**U**ndation **M**odel for **E**lectrodermal activity data), has been trained on approximately 275 million of 60-second windows of EDA data and it is, to best of our knowledge, the first EDAspecific foundation model reported in the literature. We evaluated UME on several downstream tasks and found that it surpasses baseline models trained on both generic and EDA-specific handcrafted features in 8 out of 10 tests and matches the performance of generalist time series foundation models, while requiring at least 20× less computational resources. Our results, however, also highlight the intrinsic difficulty of working with EDA signals: balanced accuracy scores rarely exceed 0.7 and exhibit substantial variability. Further research is therefore needed to fully harness the potential of EDA for both unimodal and multimodal ubiquitous sensing.

To enable further research, we make all artifacts produced as part of this work publicly available. The EDAMAME dataset collection can be obtained upon signing a single data sharing agreement, in accordance with the provisions of the individual datasets. UME’s weights and the entire codebase used to produce the model is available for download: [Link to the repository anonymized]¹.

2 Background & related work

In this section, we provide an overview of the background and relevant related work. We discuss the relevant background associated with wearable devices and EDA data. Then, we describe existing research on foundation models for physiological data, with a focus on signals collected from wearable devices. We also present work on the use of self-supervised learning applied to EDA data, since self-supervised learning is one of the main building blocks for training foundation models.

Background Foundation models require large scale datasets to be trained [14]. Researchers have obtained state-of-the-art results in the NLP domain thanks in part to the availability of large scale textual corpora, e.g., [10, 17]. Researchers create textual corpora by, for example, crawling websites and gathering all available text, e.g., as done by the Common Crawl dataset². On the other hand, collecting physiological signals requires the use of specialized equipment as well as significant human and time resources [60, 83]. Researchers have explored foundation models for physiological data through the use of large scale clinical corpora [58]. Only recent work, e.g., [1], explores the use of foundation models trained from real-world wearable physiological signals. This is due to significantly higher operational difficulties in gathering high-quality data when collecting wearable data, compared to clinical studies [13]. Additionally, EDA, even if used in the healthcare domain to detect seizures [21], is not as commonly collected in clinical settings as PPG or ECG [25, 74].

¹The link to the repository will be made available upon completion of the reviewing process

²<https://commoncrawl.org>

Table 1: Overview of selected foundation models for physiological data and the datasets used to train them.

Ref.	Foundation model			Dataset(s)	train data			Users	Avail.
	Signal(s)	Params.	Avail.		Data type	Hours (k)			
Clinical data									
[72]	PPG	~ 30 - 150 M	Open source	VitalDB [57] MIMIC-III [50] MESA [94]	Clinical Clinical Clinical	~ 17 ~ 20 ~ 20	~ 6k ~ 6k ~ 2k	✓ ✓ ✓	
[32]	PPG	~ 1-8 M	Code only	[32]	Clinical	~ 300	~ 29k	✓	
[66]	ECG	~ 300 M	Open source	MIMIC IV [51] PhysioNet2021 [78]	Clinical Clinical	~ 140 ~ 14	~ 160k N/A	✓ ✓	
[59]	ECG	~ 30M	Open source	UHN-ECG [66] HEEDB [54]	Clinical Clinical	~ 100 ~ 1,000	~ 180k ~ 2M	✓ ✓	
[84]	EEG	not stated	Open source	curated collection	Clinical	~ 350	~ 9	✗ ³	
Wearable data									
[1]	PPG ECG	~ 3M ~ 3M	Private Private	AHMS [88]	Wearable	~ 300 ~ 30	~ 141k ~ 106k	✗ ✗	
[68]	multi-modal	~ 1-100M	Private	[68]	Wearable	~ 40,000	~ 165k	✗	
[81]	PPG	~ 30M	Open source	MOODS [69]	Wearable	~ 40	~ 120	✗	
Other									
[62]	multi-modal	~ 140M	Open source	curated collection	Mixed	~ 15	N/A	✗ ³	
Ours									
Ours	EDA	~ 1M	Open source	EDAMAME	Wearable	~ 25	~ 630	✓	

Foundation models for physiological data In Table 1 we provide an overview of a selected set of existing foundation models for physiological data, their size, their availability and information about the data used to train them. Current research focuses on PPG, ECG, or multi-modal approaches. A majority of the selected foundation models relies on clinical data, given its abundance. To the best of our knowledge, Saha et al. [81]’s work is the only one using exclusively wearable physiological data to train an open source foundation model.

Researchers have explored foundation models for physiological data using both clinical and wearable data. Abbaspourazad et al. [1] were the first to use a large scale, private, dataset of wearable data to train foundation models on PPG and ECG data. Their results show that features from foundation models can be used to perform multiple downstream tasks, with performance on par to existing approaches. Following these results, other researchers, e.g., [81, 72, 32, 66, 59], have trained foundation models for either PPG or ECG data. However, most of the existing approaches rely on clinical PPG and ECG signals, with limited work on real-world physiological data collected from wearable devices [81], and, especially, no work on EDA data.

Multi-modal approaches have also recently been proposed. Narayanswamy et al. [68] trained a family of multimodal foundation models on data aggregated over 1 minute. They compute aggregated features from PPG (e.g., mean heart rate), EDA (e.g., mean EDA values), and other physiological and behavioral signals. They find that their foundation model significantly outperforms (up to 50% improvement) over baseline methods. However, their approach relies on proprietary data and the authors released neither the code nor the weights for their model. Using publicly available data, Luo et al. [62] trained a multi-modal foundation model for physiological data, e.g., PPG, ECG, EDA, from a curated collection of datasets with about 15’000 hours of data. In their experimental setup, they show promising zero-shot downstream performance for their foundation model. However, the authors’ focus was not on EDA data, which means that their collection of datasets only contained a limited amount of EDA, compared to other physiological signals. Overall, a curated EDA dataset collection has not yet been made available to the wider research community.

Self-supervised learning for EDA data Researchers have also explored the use of self-supervised learning on wearable data, including EDA. Dissanayake et al. [33] trained a self-supervised learning model, through contrastive learning, for emotion estimation using PPG, EDA and skin temperature. Saeed et al. [80] similarly used a multi-modal self-supervised approach in a federated learning settings. Recently, Matton et al.

³Individual datasets available, but not the curated collection.

[64] trained a self-supervised learning model on EDA data to perform stress classification. They used contrastive learning and data augmentation techniques to achieve state-of-the-art performance on in-distribution downstream tasks.

Overall, existing work suggests that foundation models for physiological data can be trained and used on a diverse set of downstream tasks when using PPG, ECG or multi-modal approaches. However, a large part of publicly available physiological foundation models rely on clinical data, and there is limited evidence that features from these models can be used with data from wearable devices and real-life settings. Recent work on multi-modal [62] and PPG [81] foundation models shows that, even without large-scale proprietary datasets, researchers are able to train open source foundation models. However, recent work does not provide a readily available collection of datasets for researchers to build upon their results, hindering the development of wearable foundation models. Given promising work on self-supervised learning for EDA data [64], we create a collection of datasets, EDAMAME, which we make available to the research community and, with it, we train an open source foundation model for EDA data, UME, whose code and weights we make available to the research community.

3 EDAMAME: a collection of electrodermal activity datasets

In this section, we describe how we address the availability of large scale datasets containing wearable EDA data through EDAMAME (**EDA** Multi-dataset **A**rchive for **M**odel training and **E**valuation). EDAMAME is a collection of existing, smaller scale, datasets prepared and pre-processed in a unified manner. The goal of EDAMAME is to enable researchers to train foundation models for wearable EDA data.

3.1 Description of the collection of datasets

Our goal is to create a large-scale and diverse corpus to address the scarcity of EDA-specific collections. To this end, we first identify a set of scenarios that are relevant for EDA data through relevant literature [47]. The scenarios are: *sleep monitoring*, *stress/emotion induction*, *engagement*, *real-world stress*, *workplace analysis*, *daily living*. Then, we select and search datasets from the literature using the following criteria:

1. datasets have to contain *raw* EDA data from wearable devices;
2. the individual datasets have to be either open source or available to researchers upon signing a data sharing agreement;
3. datasets have to contain data collected during tasks or moments that influence EDA signals;
4. the collection has to contain datasets collected using different protocols. e.g., lab environment or in-the-wild collection;
5. the collection needs to contain at least one dataset from each one of the six scenarios defined;
6. in order to limit the search size, we also add a saturation criterion: once we reach the threshold of 100 users and 1000 hours for one of the six scenarios, we stop searching for additional data;
7. the total size of EDAMAME has to be more than 15'000 hours and more than 100 users, which is a size similar to that of datasets used to train existing open source foundation models for wearable data [81, 62].

In order to satisfy the first criterion, we collect data only from datasets using Empatica E4 devices⁴. We choose to use only Empatica E4 data since it is one of the few research-grade wearable devices that allow to continuously collect wearable EDA.

We search datasets through open source databases containing physiological data, specifically PhysioNet⁵, Zotero⁶, Kaggle⁷. We also search for dataset information using databases of scientific articles, e.g., Google Scholar⁸, ACM Digital Library⁹. Finally, we also search through the online databases of scientific journals

⁴<https://www.empatica.com/research/e4/>

⁵<https://physionet.org/>

⁶<https://zenodo.org/>

⁷<https://www.kaggle.com>

⁸<https://scholar.google.com>

⁹<https://dl.acm.org>

Table 2: Summary of the datasets included in the training split. The collection spans diverse physiological scenarios and environments.

Dataset Name	Duration (h)	# Users	Scenario	Environment
APSync [38]	168	27	Real-world Stress	Wild
BIG IDEAS [11]	2607	16	Daily Living	Wild
BiHeartS [3]	2911	11	Sleep Monitoring	Wild
DREAMT [92]	882	100	Daily Living	Wild
Dynamics in the workplace [61]	1813	42	Workplace Analysis	Wild
EmpaticaE4Stress [20]	5	29	Stress/Emotion Induction	Lab
EPM-E4 [37]	22	47	Engagement	Wild
HeartS [2]	886	5	Sleep Monitoring	Wild
HHiSS [42]	3166	46	Real-world Stress	Wild
LAUREATE [55]	1406	46	Engagement	Wild
M2Sleep [40]	8403	16	Sleep Monitoring	Wild
MEFAR [28]	27	23	Stress/Emotion Induction	Lab
Nurses' Stress [48]	800	18	Workplace Analysis	Wild
PPG-Dalia [77]	38	15	Daily Living	Wild
SEED [29]	340	31	Engagement	Wild
SEED-II-Lab [29]	29	25	Engagement	Lab
SEED-II-Wild [29]	156	6	Engagement	Wild
Stress Predict [49]	32	35	Stress/Emotion Induction	Lab
ToadStool [85]	10	10	Stress/Emotion Induction	Lab
USILaughS [30]	1.5	30	Stress/Emotion Induction	Lab
WEEE [41]	17	17	Daily Living	Lab
WESAD [82]	29	15	Stress/Emotion Induction	Lab
WESD [75]	123	10	Real-world Stress	Wild
Workplace [31]	830	14	Workplace Analysis	Wild
Total	24'735	634		

that publish datasets containing physiological data, e.g., Nature Scientific Data¹⁰, IMWUT¹¹. We identify a potential 37 datasets. Through the aforementioned criteria, we select a total of **24** datasets for EDAMAME. We report in Table 2 an overview of the 24 datasets. In total, EDAMAME contains approximately 25'000 hours of EDA data from 634 users. The size of EDAMAME is in line, as outlined by our seventh selection criterion, with collections of datasets used by Saha et al. [81], Luo et al. [62] to train open source foundation models for wearable physiological data.

The EDA signal in all 24 datasets is sampled at 4 Hz, since this is the default sampling rate for EDA from the Empatica E4¹². All timestamps are converted to UTC time. Whenever timestamps are missing, we assign unix-time 0 to the start of a timeseries of EDA data.

3.2 Data variability in EDAMAME

In this section, we show the data variability in the EDAMAME collection of datasets. We highlight the diversity of EDA data in EDAMAME to highlight its feasibility in training foundation models for EDA data. In particular, we discuss the EDA data distribution and the distribution of users and data per user across the datasets. Figure 1 shows six example EDA signals from different datasets, representing six distinct scenarios: *sleep monitoring*, *stress/emotion induction*, *engagement*, *real-world stress*, *workplace analysis*, *daily living*.

Data distribution Figure 2 shows the distribution of raw EDA values across the 24 datasets in EDAMAME. We highlight how data distribution is similar across datasets that are collected in similar scenarios. We highlight that higher EDA values are associated with stronger ANS arousal activation [15]. For example, datasets in the *Stress/Emotion Induction* scenario have longer tails, in their distribution, compared to others. On the other hand, datasets in the *Real-world Stress* scenario have lower tails and more

¹⁰<https://www.nature.com/sdata/>

¹¹<https://dl.acm.org/journal/imwut>

¹²<https://www.empatica.com/blog/decoding-wearable-sensor-signals-what-to-expect-from-your-e4-data>

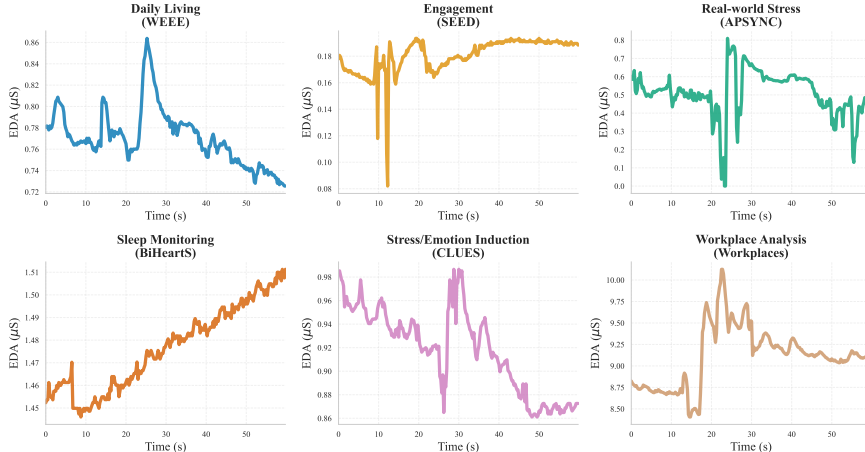


Figure 1: Example of six EDA signals (randomly drawn). Each signal is from a different dataset, each for one of the six scenarios.

EDA values close to 0 μS . These two distinct patterns highlight the challenges of real-world EDA data: a lower distribution of EDA values in the *Real-world Stress* scenario suggests that during daily life less arousal-associated moments are present. Overall, EDAMAME contains diverse data, across both scenarios and EDA values. This diversity is important when training foundation models, since it exposes the model to a wide range of EDA data.

Number of users and data per user Figure 3 shows the number of users compared to the data density per user, for each dataset in EDAMAME. The plot shows the structural topology of the collection of datasets. Specifically, the collection contains two types of datasets: datasets that contain less users but more data per user (longitudinal depth); and datasets that contain more users, but less data per user (high population diversity). The first set of datasets in which multiple days of data for each user are present contains more intra-personal variability information, i.e., how people’s data changes over time, compared to the second set. The second set, on the other hand, contains more inter-personal variability information, i.e., how data differs between different participants, compared to the first one.

EDAMAME contains data from a diverse range of scenarios and users. The collection also balances datasets with longitudinal depth and datasets with high population diversity. This diversity and variability is in line with recent literature on foundation model train data [23, 18].

4 UME: open source foundation model for EDA data

In this section, we describe UME (A foUndation Model for Electrodermal activity data), the first open source foundation model trained on wearable EDA data. In particular, we explain the data pre-processing, the training criteria, the model architecture and additional information about training the model. With UME, our objective is to obtain a model whose internal representations encode key characteristics of the input EDA signal, such that these representations can be extracted and used as substitutes for domain-informed features in downstream tasks. To achieve this objective, as common for foundation models for physiological data, e.g., [1, 72, 81], we rely on self-supervised learning with a contrastive learning objective. To train UME we use a subset of the EDAMAME collection of datasets, consisting of around 19’000 hours of EDA data and approximately 400 users. We open source the code and the weights for the model, and the EDAMAME collection of datasets is available to researchers (see section 8 for additional details). We show in Figure 4 an overview of the pipeline used to train and evaluate UME.

4.1 Data pre-processing and preparation

Data split We divide EDAMAME into two parts: a train and a downstream evaluation parts. For simplicity, we call the first EDAMAME-train and the second EDAMAME-test. We use EDAMAME-train to train our foundation model for wearable EDA data, while EDAMAME-test to perform evaluation on

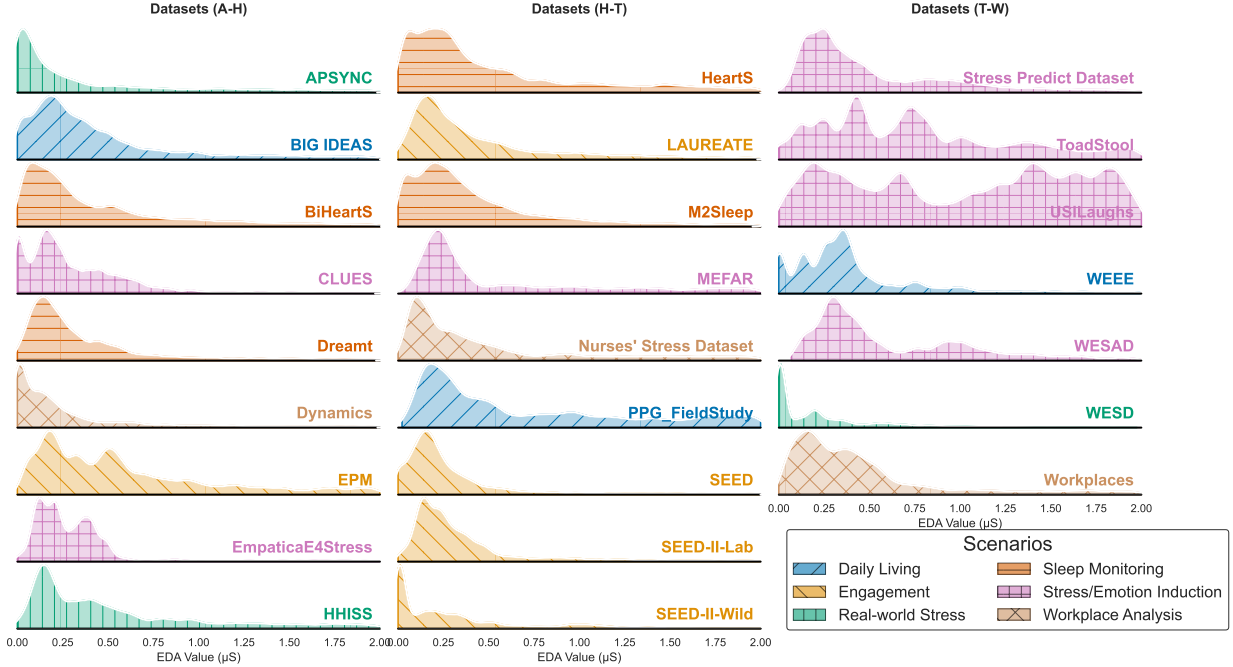


Figure 2: Ridgeline plot with distribution of EDA values from each dataset. The colors represent the six scenarios each dataset was collected in. The plot has been truncated, for visualization’s sake, in the range $0 - 2.5 \mu\text{S}$. The original range was $0 - 40 \mu\text{S}$ (the E4’s max theoretical value is $100 \mu\text{S}$).

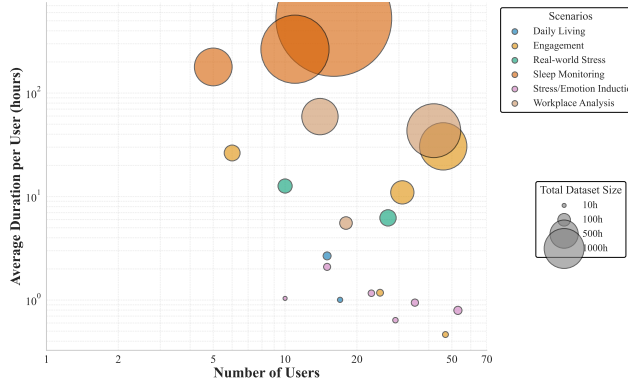


Figure 3: Number of users and data per user across the EDAMAME collection of datasets. Marker size is proportional to the size of the dataset (in terms of hours of EDA data).

a set of downstream classification tasks. We select 17 datasets for EDAMAME-train and 7 datasets for EDAMAME-test. We perform this split to allow models to be tested on data never seen during training, containing new users, locations, and protocols as well. We select the datasets in the downstream task in order to have a diverse set of labels relevant for EDA data. We report in Table 3 the binary task from each dataset in the downstream evaluation part.

Pre-processing We pre-process the data from both EDAMAME-train and EDAMAME-test parts following related work on EDA data [4, 30, 39, 46]. First, we apply a Butterworth low-pass filter (cutoff 0.4 Hz) to remove high-frequency noise. Then, we decompose the EDA signals into phasic and tonic components, using the cvxEDA method from Greco et al. [45]. This is a common procedure applied when working with EDA data. The phasic component is associated with short-term changes, e.g., momentary stress, while the tonic component with longer term variations [15]. To train the UME foundation model, we use both the phasic and tonic components, as well as the non-decomposed EDA signal. Using all three signals, i.e., phasic, tonic

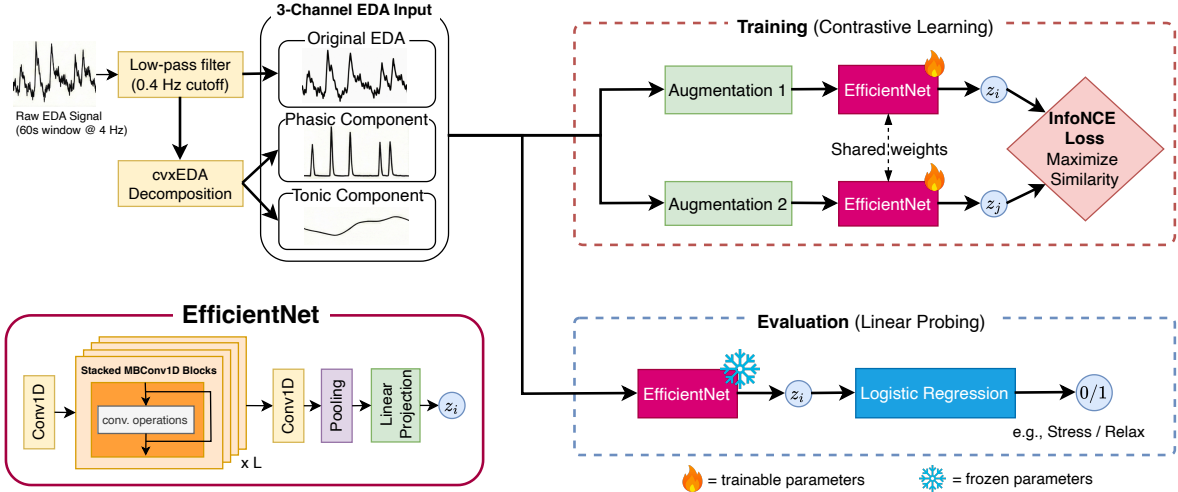


Figure 4: Overview of the train and downstream evaluation process we used for the UME foundation model. For reference, we report a sketch of the EfficientNet architecture, which we use as backbone for UME.

and original EDA signal, is a common procedure in classification-based tasks using EDA data, since it allows models to learn both short and long-term effects in the data [4, 5].

Data segmentation After pre-processing the data, we segment the EDA signals into fixed-length windows of 60 seconds. We use the same window length as Matton et al. [64] and Schmidt et al. [82], who highlight how this length allows to capture both short and long-term changes in the EDA data. To train UME, on EDAMAME-train we select maximum overlapping windows, i.e., with an overlap step of 0.25 s (the sampling rate). We implement this approach as done by Matton et al. [64], on self-supervised learning for EDA data, and Ansari et al. [8], Goswami et al. [43], Feofanov et al. [35], on generalist time series foundation models for other physiological signals. With this approach, we obtain a train set consisting of approximately 275 million windows of EDA data.

We also apply the same 60-second segmentation on the data used for evaluation, i.e., EDAMAME-test. For evaluation, we assign to each window a binary label, corresponding to the associated task: we refer to Table 3 for an overview of the binary downstream tasks used. Whenever a dataset contains EDA collected simultaneously from both sides of the body, for evaluation we use only the data from the body side most associated with the task, following guidelines by Alchieri et al. [4], e.g., right-side EDA signals for cognitive load classification. On EDAMAME-test, we use non-overlapping windows, since the literature shows how testing on either overlapping or non-overlapping windows leads to similar results [26, 87].

Discussion on rescaling the data We do not apply any normalization or standardization, e.g., min-max normalization, on the prepared windows of EDA data. Researchers working with EDA data collected in lab-controlled environments apply per-user min-max normalization to reduce inter-personal variability and improve classification performance significantly, e.g., [67, 82, 7]. However, EDA data is affected by both inter-personal variability, which min-max normalization addresses, and intra-personal variability, i.e., a user’s data changes over time. A fix calibration, like the one applied by min-max normalization, is rendered invalid over time if a user’s signal morphology changes [91, 12]. Moreover, “cold-start” approaches, i.e., a machine learning model is applied directly on a new user, are the preferred approach for wearable physiological data [93]. Normalization approaches cannot be implemented directly in “cold-start” scenarios.

4.2 Model training task & architecture

Training objective We adopt contrastive learning to train UME. Contrastive learning is used by multiple researchers to train foundation models for wearable physiological data, e.g., [1, 72]. This approach has also been used for generalist time series foundation models specialized in classification tasks, e.g., [35]. Contrastive learning is a self-supervised learning method that consists in training an encoder-only model to learn a latent embedding space where representations of similar data pairs — typically created via augmentations of the

Table 3: Summary of Datasets and Associated Binary Tasks

Dataset	Binary Tasks
APSync	Low/High Engagement
HeartS	Sleep/Wake
USILaugh	Cog. Load/Relaxation
WESAD	High/Low Arousal, High/Low Valence (self-report)
Nurses' Stress	Low/High Stress
DREAMT	Sleep/Wake
HHS	Low/High Stress

same signal — are attracted to each other, while representations of dissimilar pairs are repelled. The latent embeddings often contain information which allows them to be used effectively in downstream tasks [56]. We also experiment with an additional self-supervised learning method: masked reconstruction. This method consists in training an encoder-decoder to reconstruct the whole signal from a masked version of it, i.e., a signal which is missing some parts. We report in Appendix B details about this additional experiment which, however, failed to learn useful representations of our EDA data.

Model architecture We choose the architecture for our foundation model from similar work in the literature [1, 68, 72, 35]. Our choice reflects the decision to implement a generalist time series foundation model on EDA data. This choice is in line with research on the first PPG and ECG-specific foundation models [1, 68]: our objective is to showcase how features computed from EDA-specific foundation models perform, as well to provide weights and code to the research community. Each physiological signal, from PPG to ECG and EDA, has morphological elements specific to them. It is possible to define architectures for foundation models that adapt to these morphological elements, as recent work from Saha et al. [81] show. However, this implementation goes beyond the scope of the current work.

We chose an EfficientNet [86] architecture, as Abbaspourazad et al. [1], since it is computationally less expensive than traditional CNN backbones. We consider this choice also in light of the fact that foundation models for wearable data have the potential to be used on wearable devices themselves [1]. We adapt the EfficientNet for our input data, i.e., 1-dimensional time series data of 240 values (60 s at 4 Hz) with 3 channels (tonic, phasic and original EDA signal). We report in Appendix B ablation studies on the model size and hyperparameters. We implement a version of EfficientNet with approximately 1M parameters and a latent representation of $d = 64$.

4.3 Training process

Train loss Using the contrastive learning training objective and EfficientNet architecture defined in subsection 4.2, we train UME using the InfoNCE loss [89]. Formally, for a given pair of embeddings (z_i, z_j) , the loss is defined as:

$$\mathcal{L}_{i,j} = -\log \frac{\exp(\text{sim}(z_i, z_j)/\tau)}{\sum_{k=1}^{2N} \mathbb{1}_{[k \neq i]} \exp(\text{sim}(z_i, z_k)/\tau)} \quad (1)$$

where $\text{sim}(\cdot, \cdot)$ denotes the cosine similarity, $\tau = 0.1$ is a temperature hyperparameter, N is the batch size, and $\mathbb{1}$ is the indicator function. This objective maximizes the similarity between representations of the same underlying signal while minimizing agreement with unrelated samples.

Pairs of EDA data We generate positive pairs of EDA signals by applying two distinct stochastic augmentations to the same EDA signal segment (an anchor segment). We employ the set of data augmentations optimized for EDA signals proposed by Matton et al. [64]. Negative pairs consist of comparisons between the anchor segment and all other segments in the mini-batch. This set combines both standard data augmentation techniques (e.g., signal warping) and augmentations specific to EDA data (e.g., loose sensor artifact). We report the complete list of augmentations and additional details about the training in Appendix A (Table A.5).

5 Evaluation of UME

In this section, we report the results of the evaluation procedure of UME on the selected downstream tasks from EDAMAME-test. We use *linear probing* with frozen weights to evaluate the performance on the selected classification tasks, as frequently done to evaluate performance of foundation models [1, 81, 72, 95]. We compare the UME feature set to various baseline features, including generic handcrafted features, a set of EDA-specific features, and features computed from generalist time series foundation models. Finally, we also evaluate the computation complexity of the UME foundation model in extracting features, computed to the other baseline methods.

5.1 Experimental evaluation setup

Evaluation through linear probing We evaluate the features computed from the UME foundation model using *linear probing* on the downstream tasks from EDAMAME-test. For each dataset, we freeze the trained weights from the foundation model to compute features on the EDA data. Then, we train a logistic regression classifier on the computed feature set. The usage of frozen weights and linear probing is commonly done in similar work on foundation models for physiological data [1, 72, 81]. We use the same evaluation procedure for UME and the other baseline features sets. We use a linear model for all approaches since we are gauging the representativeness of the features sets on classification tasks, and not that of the downstream model itself. Linear probing also allows to estimate the linear separability of the different feature sets.

Cross-validation protocols for the downstream tasks We evaluate the linear probing using two distinct cross-validation methods. The first method is Leave-One-Participant-Out (LOPO) cross-validation. LOPO cross-validation is used by researchers to evaluate how machine learning models generalize to new users [76]. With this method, we test robustness to inter-personal variability. The second validation method is Time-Aware (TA) cross-validation [6], which we use to evaluate the model’s ability to generalize to data from users already seen in the train set, and this we test robustness to intra-personal variability. We partition users into N folds: the model trains on all external groups plus the first chronological $2/3$ of the target fold, reserving the final $1/3$ of data strictly for testing. This approach simulates a realistic scenario where a model uses a specific participant’s historical data to predict their future states. In our experimental setup, we use $N = 5$.

In both validation methods, we perform hyperparameter tuning for the logistic regression at train set, i.e., at each cross-validation iteration. We perform hyperparameter selection using a 3-fold “inner” cross-validation with grid search. We report in Appendix A information about the hyperparameter grid used.

Baseline feature sets We compare the performance using linear probing on the features computed from UME and using other baseline methods. Specifically, to follow the same experimental setup of similar work on foundation models for physiological data [1, 72, 68], we define a set of baseline, *generic*, handcrafted features. These features are: the mean, the standard deviation, the minimum and the maximum of a 60 s EDA signal. We compute these features for all three EDA components, i.e., phasic, tonic and original signal. In total, the dimensionality of this feature set is $d = 12$.

However, the aforementioned generic handcrafted feature set does not represent the state-of-the-art approach for EDA-based classification tasks [4, 39, 63]. To this end, we also implement a second handcrafted feature set, which we call *EDA-specific* handcrafted features. This feature set includes both statistics, e.g., average of the first derivative, as well as feature specific to EDA data, e.g., number of EDA peaks and their average amplitude. As with the generic handcrafted feature set, we compute these features on 60 s windows and for all three EDA components. In total, the EDA-specific handcrafted features are $d = 45$.

We also compare the performance using linear proving of the feature set from UME with other generalist time series foundation models. We compare with the following: Chronos [8], MOMENT [43] and Mantis [35]. We select these three foundation models since Alchieri et al. [5] show how they achieve performance similar to the EDA-specific handcrafted features when using EDA data. Saha et al. [81] also show that Chronos [8] and MOMENT [43] achieve, on average, performance similar to their PPG-specific foundation model on the downstream tasks selected by the authors. We also select the recent foundation model Mantis [35] since it is trained specifically for classification tasks on time series data.

Mantis takes time series of length 512 as input: we oversample our time series, which have length of 240, to match this desired length. From a single time series, Mantis computes a set of embeddings, similarly to our foundation model. Mantis has a feature set size of $d = 768$ (embedding size of 256 across three channels).

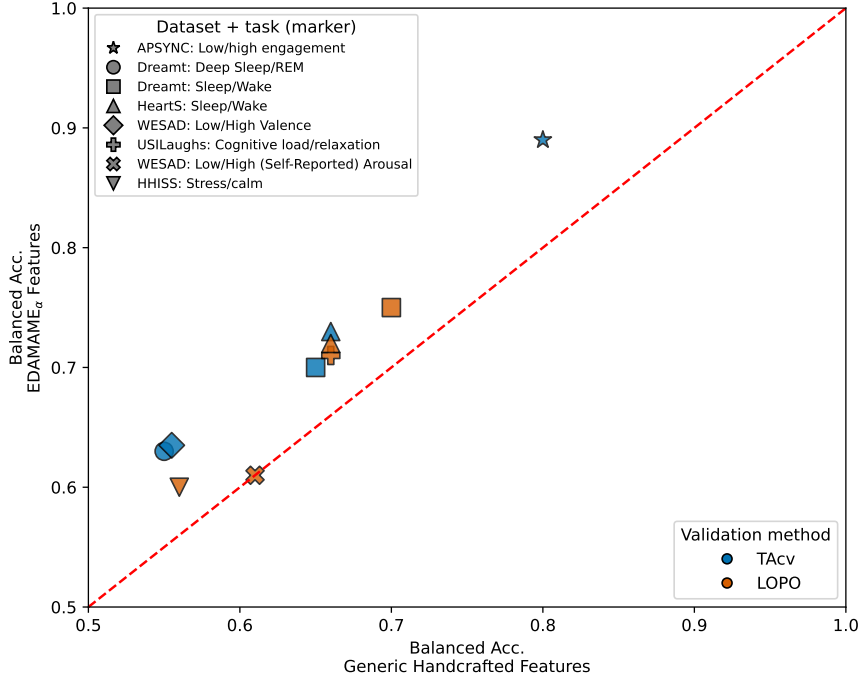


Figure 5: Pairplot with comparison between UME and the baseline features for the selected downstream tasks. Colors represent the two validation methods, TA and LOPO.

The embedding size of MOMENT is $d = 1024$. However, Chronos computes embeddings ($d = 512$) for each timepoint in the series. This leads, with our input, to high dimensionality of the data. To address the high dimensionality problem, we average across the time axis the embeddings extracted from each timepoint. Overall, the feature set from Chronos is of size $d = 1536$ (embedding size of 512 across three channels).

Reporting and task selection information We report all results in terms of *balanced accuracy*. We use this metric since the downstream evaluation datasets we use contain binary labels which, in a subset of cases, are imbalanced. Balanced accuracy accounts for class imbalance, reporting results which are more representative of the real performance on a specific task [16, 70]. At the same time, compared to other metrics for imbalanced data, e.g., Matthew’s correlation coefficient (MCC), balanced accuracy is more interpretable [44].

In addition to the results from the identified feature sets, we also report results from a dummy classifier. The dummy classifier reported is the one achieving the highest balanced accuracy in each given task, among the following: *most frequent*, which predicts always the most frequent class set; *uniform*, which predicts the binary labels by drawing randomly from a uniform distribution; and *prior*, which predicts the binary labels by drawing randomly from the distribution of labels in the train set.

We report in this section results from tasks that are *solvable*, i.e., at least one feature set achieves balanced accuracy higher than the dummy classifier. If no model achieves balanced accuracy higher than, for example, random chance, we conclude that it is not due to issues with the feature sets, but with the task itself, e.g., the task is not solvable with the given constraints.

5.2 Comparison with generic handcrafted feature set

We present in Figure 5 the comparison when performing linear probing on the selected downstream tasks, between the feature set from our UME foundation model and the generic handcrafted features. We show results for both validation methods, i.e., LOPO and TA. The results show that the features from our foundation model outperform the generic handcrafted features in 9 out of 10 tasks. The improvement holds true regardless of the scenario and the task selected. We conclude from these findings that the UME foundation model learns features useful for EDA data in performing downstream predictions. Our findings are in line with works on foundation models for PPG, when comparing to generic handcrafted feature sets [1, 72, 68].

5.3 Comparison with other baseline feature sets

We report in Table 4 the results for the evaluation of our UME foundation model, in terms of balanced accuracy and for two distinct validation methods, i.e., Time-Aware (TA) cross-validation and Leave-One-Participant-Out (LOPO) cross-validation. We compare the feature set computed using UME to the following feature sets: a set of generic handcrafted features; a set of EDA-specific handcrafted features; and features computed using generalist time series foundation models, specifically Mantis [35], Chronos [8] and MOMENT [43].

Results using TA The TA method tests the intra-personal generalizability of models trained using the different feature sets, i.e., the ability to generalize to new data from users already seen in the train data. Our first finding is that, using linear probing, models trained using features from UME always outperform non-foundation model methods, i.e., both generic and EDA-specific handcrafted features. We conclude that the embeddings from UME capture user-specific dynamics, which allow to obtain a balanced accuracy on par, or higher, than handcrafted-based methods. We also find that models trained using the feature set from Mantis [35], which is trained to solve generic classification tasks, perform similarly to those trained using the feature set from UME. We notice how the other two foundation models, MOMENT [43] and Chronos [8], have lower performance, on a majority of tasks, than both the two handcrafted feature sets and the foundation models (UME and Mantis [35]).

Results using LOPO The LOPO cross-validation method tests the inter-personal generalizability of models trained using the different feature sets, i.e., the ability to generalize to data from new users not seen in the train set. We find that models trained from the UME features have similar balanced accuracy to models trained from either the EDA-specific handcrafted features and the embeddings computed using Mantis [35]. Features from the other foundation models have similar or lower performance as well. Generalization to new users is a known issue when working with EDA data [39]. While features from foundation models, both our model and others, achieve performance similar to that of EDA-specific handcrafted features, they do not solve the “cold-start” problem.

Additional remarks on standard errors We highlight how, regardless of the feature set used, the standard error associated with all results leads to overlapping confidence intervals. In other words, while there are trends, e.g., models trained using features from UME outperforming models trained using EDA-specific handcrafted features in a majority of tasks, there is no statistical difference between results obtained using the different feature sets. However, all results are statistically higher (t-test corrected with Bonferroni) compared to the results obtained using the dummy classifier.

Result analysis using Friedman-Nemenyi test We perform the Friedman test, followed by the post-hoc Nemenyi test, to compare model performance across all experiments [27]. We consider each combination of dataset-validation method as a single sample for the statistical analysis. The Friedman test is used to determine whether *any* statistical difference is present across all models and experiments. For the Friedman test, we find a p-value of approximately 0.0001, which is below the reference threshold of $\alpha = 0.05$. We conclude from this result that, across all experiments, there are statistically significant differences. In particular, we attribute this finding to the difference between all methods, i.e., both handcrafted- and foundation model-based, and the dummy classifier baseline. We use the post-hoc Nemenyi test to perform pair-wise statistical comparisons, from the model rankings provided by the Nemenyi test. We report the findings with respect to our UME foundation model only. We refer to the Appendix B to additional results. First, we find that our method achieves performance statistically higher than the dummy classifier baseline ($p = 0.02 < \alpha = 0.05$). Secondly, we find that the performance difference in linear probing between feature sets computed using UME and Mantis [35] is not statistically different ($p \simeq 0.9 > \alpha > 0.05$). Finally, we also find no statistical difference between using our UME and the EDA-specific handcrafted features ($p \simeq 0.9 > \alpha = 0.05$).

From the Friedman-Nemenyi test findings, we conclude that both our UME and Mantis [35] capture time series dynamics which allow to achieve, on average, performance similar to the EDA-specific handcrafted feature sets. Our EDA-trained foundation model performs on-par with a large-scale generalist time series foundation model, Mantis [35], even if trained on a relatively smaller dataset and with fewer parameters (1M ours vs 8M Mantis).

Table 4: Results of binary classification experiments across datasets and tasks, in terms of *balanced accuracy*_{standard error}. Reported are results for both TA and LOPO cross-validation methods. Acronyms: *Gen. HC* stands for *generic handcrafted features*; *EDA HC* stands for *EDA-specific handcrafted features*.

Dataset	Binary Task	Dummy	Handcrafted (HC)		Generalist Foundation			Ours
			Gen.	EDA-spec.	Mantis	MOMENT	Chronos	UME
<i>Balanced accuracy</i> _{standard error}								
Time-Aware cross-validation (TA)								
APSYNC	Low/High engagement	.45 _{.20}	.80 _{.10}	.80 _{.10}	.86 _{.07}	.47 ₁₆	.61 _{.20}	.89 _{.11}
Dreamt	Deep Sleep/REM	.48 _{.02}	.55 _{.05}	.59 _{.04}	.64 _{.03}	.65 ₀₁	.63 ₀₂	.63 _{.05}
Dreamt	Sleep/Wake	.50 _{.01}	.65 _{.02}	.69 _{.01}	.73 _{.01}	.69 ₀₁	.73 ₀₁	.70 _{.01}
HeartS	Sleep/Wake	.49 _{.00}	.66 _{.04}	.72 _{.07}	.75 _{.09}	.69 ₀₆	.74 ₀₆	.73 _{.09}
WESAD	Low/High Valence	.51 _{.03}	.55 _{.10}	.54 _{.10}	.61 _{.04}	.64 ₀₅	.45 _{.06}	.63 _{.06}
Leave-one-participant-out (LOPO) cross-validation								
Dreamt	Sleep/Wake	.48 _{.00}	.70 _{.01}	.74 _{.01}	.76 ₀₁	.73 ₀₁	.78 ₀₁	.75 _{.01}
USILaughS	Cog. load/relax	.50 _{.00}	.66 _{.03}	.70 _{.04}	.72 _{.05}	.60 _{.05}	.67 _{.03}	.71 _{.05}
HeartS	Sleep/Wake	.50 _{.00}	.66 _{.04}	.70 _{.03}	.74 _{.03}	.70 _{.02}	.73 _{.03}	.72 _{.03}
WESAD	Low/High Arousal	.58 _{.05}	.61 _{.04}	.63 _{.04}	.56 _{.04}	.66 _{.04}	.66 _{.05}	.61 _{.05}
HHiSS	Stress/calm	.50 _{.00}	.56 _{.02}	.64 _{.01}	.63 _{.02}	.55 _{.01}	.59 _{.01}	.60 _{.02}

5.4 Computational complexity analysis

We compare the computational complexity of the different feature extraction methods, i.e., the handcrafted-based approaches, our UME foundation model, and the other baseline foundation models. We compare the methods using both *CPU execution time* and FLOPs [22]. We choose this dual approach since handcrafted features cannot be compared using FLOPs alone. We perform all calculations using an Apple M1 Max CPU.

To get *CPU execution time*, we use a random subset of twenty 60 s windows from the downstream part of the UME collection. We also use additionally three samples per experiment as warm-up runs. We perform FLOPs computation using the `fvcore` Python library. We report in Figure 6 the results. We find that the handcrafted feature extraction methods have the lowest CPU execution time, as expected. We also find that our UME foundation model is significantly faster than all other foundation models, both with respect to *CPU execution time* and FLOPs. We conclude that our model, which is trained specifically only on EDA data, achieves performance on-par with larger, general purpose, foundation models on a set of downstream tasks using EDA data, as detailed in subsection 5.3. However, it does so with a fraction of the computation resources needed, while also eliminating the need for expert-designed or handcrafted features, unlike traditional feature-based pipelines

6 Discussion, limitations and future work

Summary of results Through this paper, we provide the research community with the EDAMAME collection of datasets, which enabled the development of UME, the first open-source foundation model for wearable EDA. We find that UME, trained on a subset of the EDAMAME collection using contrastive

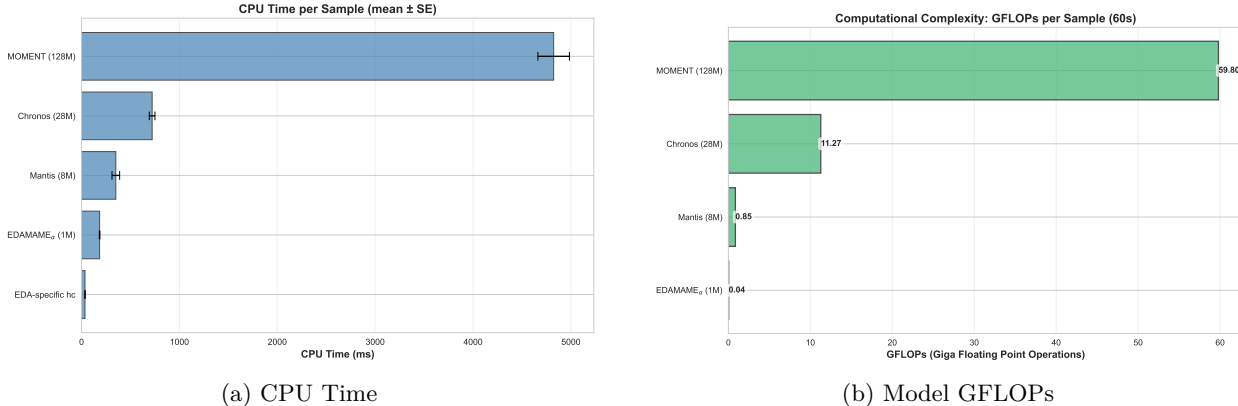


Figure 6: Computational complexity analysis. (a) Average (across 20 samples) per-sample computation time for a 60-second window of EDA data for all three components (phasic, tonic, and original signal). Note: *hc* stands for *handcrafted*; generic handcrafted features are not shown as they require negligible computation time. (b) GFLOPs for the different foundation models.

learning, surpasses the performance obtainable using both generic and EDA-handcrafted features in 8 out of 10 downstream tasks. Further, UME matches the performance of larger and much less computationally efficient generalist foundation models for time series data. By relying on publicly available data only and by releasing all artifacts produced as part of this work, we aim at fostering further research on foundation models for wearable EDA as well as other research related to unimodal and multimodal EDA sensing and modelling.

Discussion Overall, we observe that features computed using UME, generalist time-series foundation models, and EDA-specific handcrafted features lead to comparable downstream performance. It can be argued that other methodologies, in particular the use of domain-specific architectures elements, may yield superior performance. However, we believe that our results are not bound to UME’s specific characteristics, because UME’s performances not only matches those of generalist foundation models, but also often surpasses results obtained relying on EDA-specific handcrafted features. This suggests that other methodological approaches alone may yield incremental rather than substantial gains.

Instead, we believe that the reported results, obtained by UME and other methods, are close to the intrinsic upper limit reachable for the considered downstream tasks, due to the arguably limited information in the input signal that is predictive of the label. Potential additional gains can however be obtained by coping with the significant label noise and signal noise of EDA data. Wearable EDA is noisy, strongly affected by motion/contact artifacts and low signal-to-noise ratio, in particular when collected in the wild [39]. Additionally, high-level constructs (e.g., stress, engagement, valence) might only be weakly identifiable from EDA alone resolution without additional context. We believe that this represents an important direction for future work, e.g., by quantifying the impact of signal quality filtering, label reliability, and more.

A further element to highlight is that UME, which is specialized for EDA data, requires far fewer parameters to match the performance on downstream tasks of larger generalist models. As highlighted by Abbaspourazad et al. [1], developing foundation models for wearable data includes considering the usage of these models on actual wearable devices, which are resource constrained. We speculate that our results showcase how specializing foundation models for EDA data limit their size and, consequently, prospect their usage on wearable devices.

Limitations & future work We create the EDAMAME collection leveraging data collected exclusively using the Empatica E4 device. Considering data collected from a specific device removes hardware-specific domain shifts, ensuring that foundation models can learn physiological patterns rather than sensor differences. Nonetheless, future work could focus on expanding EDAMAME with data from other devices, e.g., the newer Empatica Embrace Plus¹³.

¹³<https://www.empatica.com/embraceplus>

In our pre-processing approach, we apply standard low-pass filtering and decomposition of the EDA signals using the cvxEDA method [45]. Alternative filtering or decomposition techniques [90] can be explored in future research.

Lastly, we acknowledge that the EDAMAME collection of datasets is affected by the same user and domain bias associated with the individual datasets.

7 Conclusions

In conclusion, in this work we present EDAMAME, a large scale collection of datasets containing wearable EDA data. EDAMAME, which is composed of 24 datasets, contains approximately 25'000 hours of EDA data from about 630 users. With its diversity and variability, it enables the training of foundation models for EDA data, as we show with the training of UME, the first foundation model for wearable EDA. We also make EDAMAME available to other researchers, to spur development of further foundation models.

Through a comprehensive set of experiments, we show that the latent representations obtained using UME outperform a set of generic handcrafted features when using linear probing on 9 out of 10 downstream tasks, as done in similar work in the literature [1, 72]. We also find that UME’s features achieve performance on-par with specialized EDA features and large-scale generalist foundation models, in the same set of downstream tasks. However, compared to generalist models like Chronos [8] or Mantis [35], UME is computationally lighter, e.g., $20\times$ less demanding than the smallest generalist foundation model tested, enabling its possible usage on real-world wearable devices.

We hope that this work enables researchers to further develop EDA, a sensor not (yet) as common as others like PPG on wearable devices, through both the EDAMAME collection of datasets and the open source and weights UME foundation model for wearable EDA data.

8 Dataset and code availability

We make the EDAMAME available to other researchers, *upon completion of the review process underway*. 11 datasets have an open source license which allows for re-sharing of the data under the original conditions: we re-share them, prepared in a unified format, following the original license. 11 datasets need a data sharing agreement to be accessed: we contacted the original authors, who all agreed to re-sharing under a single data sharing agreement, which includes all of the original limitations. Finally, two datasets can only be accessed through their authors: we provide the code to process them in the same format as we did. We report information about the original licenses in Appendix A (Table A.1). We will also share the code to process these datasets *after the ongoing review process*.

We also make the code to train and evaluate the UME foundation model available as open source to other researchers, as well as the model weights. The link will be provided *after the ongoing review process*.

References

- [1] Salar Abbaspourazad, Oussama Elachqar, Andrew C Miller, Saba Emrani, Udhyakumar Nallasamy, and Ian Shapiro. Large-scale Training of Foundation Models for Wearable Biosignals. In *International Conference on Learning Representations*, Vienna, Austria, 2024. International Conference on Learning Representations (ICLR).
- [2] Nouran Abdalazim, Joseba Aitzol Arbilla Larraza, Leonardo Alchieri, Lidia Alecci, Silvia Santini, and Shkurta Gashi. Heart Rate During Sleep Measured Using Finger-, Wrist- and Chest-Worn Devices: A Comparison Study. In Athanasios Tsanas and Andreas Triantafyllidis, editors, *Pervasive Computing Technologies for Healthcare*, pages 18–32, Cham, 2023. Springer Nature Switzerland. ISBN 978-3-031-34586-9. doi: 10.1007/978-3-031-34586-9_2.
- [3] Nouran Abdalazim, Leonardo Alchieri, Lidia Alecci, Pietro Barbiero, and Silvia Santini. The Impact of Domain Shift on Predicting Perceived Sleep Quality from Wearables. *Sensors*, 25(13):4012, January 2025. ISSN 1424-8220. doi: 10.3390/s25134012.
- [4] Leonardo Alchieri, Nouran Abdalazim, Lidia Alecci, Shkurta Gashi, Martin Gjoreski, and Silvia Santini. Lateralization Effects in Electrodermal Activity Data Collected Using Wearable Devices. *Proc. ACM Interact. Mob. Wearable Ubiquitous Technol.*, 8(1):2:1–2:30, March 2024. doi: 10.1145/3643541.
- [5] Leonardo Alchieri, Lino Candian, Nouran Abdalazim, Lidia Alecci, Giovanni De Felice, and Silvia Santini. Exploring Generalist Foundation Models for Time Series of Electrodermal Activity Data. In *Companion of the 2025 ACM International Joint Conference on Pervasive and Ubiquitous Computing*, UbiComp Companion ’25, pages 885–892, New York, NY, USA, December 2025. Association for Computing Machinery. ISBN 979-8-4007-1477-1. doi: 10.1145/3714394.3756186.
- [6] Leonardo Alchieri, Vittoria Scocco, Nouran Abdalazim, Lidia Alecci, and Silvia Santini. Improving Human Behavior Recognition Using Bilateral Electrodermal Activity Data Collected From Wearable Devices. In *2025 International Conference on Activity and Behavior Computing (ABC)*, pages 1–10, Al Ain, United Arab Emirates, April 2025. IEEE. doi: 10.1109/ABC64332.2025.11118532.
- [7] Ahmad Almadhor, Gabriel Avelino Sampedro, Mideth Abisado, Sidra Abbas, Ye-Jin Kim, Muhammad Attique Khan, Jamel Baili, and Jae-Hyuk Cha. Wrist-Based Electrodermal Activity Monitoring for Stress Detection Using Federated Learning. *Sensors*, 23(8):3984, January 2023. ISSN 1424-8220. doi: 10.3390/s23083984.
- [8] Abdul Fatir Ansari, Lorenzo Stella, Ali Caner Turkmen, Xiyuan Zhang, Pedro Mercado, Huibin Shen, Oleksandr Shchur, Syama Sundar Rangapuram, Sebastian Pineda Arango, Shubham Kapoor, Jasper Zschiegner, Danielle C. Maddix, Hao Wang, Michael W. Mahoney, Kari Torkkola, Andrew Gordon Wilson, Michael Bohlke-Schneider, and Bernie Wang. Chronos: Learning the Language of Time Series. *Transactions on Machine Learning Research*, May 2024. ISSN 2835-8856.
- [9] Abdul Fatir Ansari, Oleksandr Shchur, Jaris Küken, Andreas Auer, Boran Han, Pedro Mercado, Syama Sundar Rangapuram, Huibin Shen, Lorenzo Stella, Xiyuan Zhang, Mononito Goswami, Shubham Kapoor, Danielle C. Maddix, Pablo Guerron, Tony Hu, Junming Yin, Nick Erickson, Prateek Mutalik Desai, Hao Wang, Huzefa Rangwala, George Karypis, Yuyang Wang, and Michael Bohlke-Schneider. Chronos-2: From Univariate to Universal Forecasting, October 2025.
- [10] Project Apertus, Alejandro Hernández-Cano, Alexander Hägele, Allen Hao Huang, Angelika Romanou, Antoni-Joan Solergibert, Barna Pasztor, Bettina Messmer, Dhia Garbaya, Eduard Frank Ādurech, Ido Hakimi, Juan García Giraldo, Mete Ismayilzada, Negar Foroutan, Skander Moalla, Tiancheng Chen, Vinko Sabolčec, Yixuan Xu, Michael Aerni, Badr AlKhamissi, Inés Altemir Mariñas, Mohammad Houssein Amani, Matin Ansaripour, Ilia Badanin, Harold Benoit, Emanuela Boros, Nicholas Browning, Fabian Bösch, Maximilian Böther, Niklas Canova, Camille Challier, Clement Charmillot, Jonathan Coles, Jan Deriu, Arnout Devos, Lukas Drescher, Daniil Dzenhaliou, Maud Ehrmann, Dongyang Fan, Simin Fan, Silin Gao, Miguel Gila, María Grandury, Diba Hashemi, Alexander Hoyle, Jiaming Jiang, Mark Klein, Andrei Kucharavy, Anastasiia Kucherenko, Frederike Lübeck, Roman Machacek, Theofilos Manitaras, Andreas Marfurt, Kyle Matoba, Simon Matrenok, Henrique Mendonça, Fawzi Roberto Mohamed, Syrielle Montariol, Luca Mouchel, Sven Najem-Meyer, Jingwei Ni, Gennaro Oliva, Matteo Pagliardini, Elia Palme, Andrei Panferov, Léo Paoletti, Marco Passerini, Ivan Pavlov, Auguste Poiroux, Kaustubh Ponskshe, Nathan Ranchin, Javi Rando, Mathieu Sauser, Jakhongir Saydaliev, Muhammad Ali Sayfiddinov, Marian Schneider, Stefano Schuppli, Marco Scialanga, Andrei Semenov, Kumar Shridhar, Raghav Singhal, Anna Sotnikova, Alexander Sternfeld, Ayush Kumar Tarun, Paul Teiletche, Jannis Vamvas, Xiaozhe Yao, Hao Zhao, Alexander Ilic, Ana Klimovic, Andreas Krause, Caglar Gulchere,

- David Rosenthal, Elliott Ash, Florian Tramèr, Joost VandeVondele, Livio Veraldi, Martin Rajman, Thomas Schulthess, Torsten Hoefler, Antoine Bosselut, Martin Jaggi, and Imanol Schlag. Apertus: Democratizing Open and Compliant LLMs for Global Language Environments, December 2025.
- [11] Brinnae Bent, Peter J. Cho, Maria Henriquez, April Wittmann, Connie Thacker, Mark Feinglos, Matthew J. Crowley, and Jessilyn P. Dunn. Engineering digital biomarkers of interstitial glucose from noninvasive smartwatches. *npj Digital Medicine*, 4(1):89, June 2021. ISSN 2398-6352. doi: 10.1038/s41746-021-00465-w.
- [12] Andrew Beten, Luna Lococco, Ayaan Baig, and Thilini Karunaratna. Systematic Analysis of Distribution Shifts in Cross-Subject Glucose Prediction Using Wearable Physiological Data. *Engineering Proceedings*, 118(1):88, 2025. ISSN 2673-4591. doi: 10.3390/ECSA-12-26583.
- [13] Andrea Bizzego, Giulio Gabrieli, Cesare Furlanello, and Gianluca Esposito. Comparison of Wearable and Clinical Devices for Acquisition of Peripheral Nervous System Signals. *Sensors (Basel, Switzerland)*, 20(23):6778, November 2020. ISSN 1424-8220. doi: 10.3390/s20236778.
- [14] Rishi Bommasani, Drew A. Hudson, Ehsan Adeli, Russ Altman, Simran Arora, Sydney von Arx, Michael S. Bernstein, Jeannette Bohg, Antoine Bosselut, Emma Brunskill, Erik Brynjolfsson, Shyamal Buch, Dallas Card, Rodrigo Castellon, Niladri Chatterji, Annie Chen, Kathleen Creel, Jared Quincy Davis, Dora Demszky, Chris Donahue, Moussa Doumbouya, Esin Durmus, Stefano Ermon, John Etchemendy, Kawin Ethayarajh, Li Fei-Fei, Chelsea Finn, Trevor Gale, Lauren Gillespie, Karan Goel, Noah Goodman, Shelby Grossman, Neel Guha, Tatsunori Hashimoto, Peter Henderson, John Hewitt, Daniel E. Ho, Jenny Hong, Kyle Hsu, Jing Huang, Thomas Icard, Saahil Jain, Dan Jurafsky, Pratyusha Kalluri, Siddharth Karamcheti, Geoff Keeling, Fereshte Khani, Omar Khattab, Pang Wei Koh, Mark Krass, Ranjay Krishna, Rohith Kuditipudi, Ananya Kumar, Faisal Ladhak, Mina Lee, Tony Lee, Jure Leskovec, Isabelle Levent, Xiang Lisa Li, Xuechen Li, Tengyu Ma, Ali Malik, Christopher D. Manning, Suvir Mirchandani, Eric Mitchell, Zanele Munyikwa, Suraj Nair, Avanika Narayan, Deepak Narayanan, Ben Newman, Allen Nie, Juan Carlos Niebles, Hamed Nilforoshan, Julian Nyarko, Gray Ogut, Laurel Orr, Isabel Papadimitriou, Joon Sung Park, Chris Piech, Eva Portelance, Christopher Potts, Aditi Raghunathan, Rob Reich, Hongyu Ren, Frieda Rong, Yusuf Roohani, Camilo Ruiz, Jack Ryan, Christopher Ré, Dorsa Sadigh, Shiori Sagawa, Keshav Santhanam, Andy Shih, Krishnan Srinivasan, Alex Tamkin, Rohan Taori, Armin W. Thomas, Florian Tramèr, Rose E. Wang, William Wang, Bohan Wu, Jiajun Wu, Yuhuai Wu, Sang Michael Xie, Michihiro Yasunaga, Jiaxuan You, Matei Zaharia, Michael Zhang, Tianyi Zhang, Xikun Zhang, Yuhui Zhang, Lucia Zheng, Kaitlyn Zhou, and Percy Liang. On the Opportunities and Risks of Foundation Models, July 2022.
- [15] Wolfram Boucsein. *Electrodermal Activity*. Electrodermal Activity, 2nd Ed. Springer Science + Business Media, New York, NY, US, 2012. ISBN 978-1-4614-1125-3 978-1-4614-1126-0. doi: 10.1007/978-1-4614-1126-0.
- [16] Kay Henning Brodersen, Cheng Soon Ong, Klaas Enno Stephan, and Joachim M. Buhmann. The Balanced Accuracy and Its Posterior Distribution. In *2010 20th International Conference on Pattern Recognition*, pages 3121–3124, Istanbul, Turkey, August 2010. IEEE. doi: 10.1109/ICPR.2010.764.
- [17] Tom Brown, Benjamin Mann, Nick Ryder, Melanie Subbiah, Jared D Kaplan, Prafulla Dhariwal, Arvind Neelakantan, Pranav Shyam, Girish Sastry, Amanda Askell, Sandhini Agarwal, Ariel Herbert-Voss, Gretchen Krueger, Tom Henighan, Rewon Child, Aditya Ramesh, Daniel Ziegler, Jeffrey Wu, Clemens Winter, Chris Hesse, Mark Chen, Eric Sigler, Mateusz Litwin, Scott Gray, Benjamin Chess, Jack Clark, Christopher Berner, Sam McCandlish, Alec Radford, Ilya Sutskever, and Dario Amodei. Language Models are Few-Shot Learners. In *Advances in Neural Information Processing Systems*, volume 33, pages 1877–1901, Online, 2020. Curran Associates, Inc.
- [18] Alexander Bukharin, Shiyang Li, Zhengyang Wang, Jingfeng Yang, Bing Yin, Xian Li, Chao Zhang, Tuo Zhao, and Haoming Jiang. Data Diversity Matters for Robust Instruction Tuning. In Yaser Al-Onaizan, Mohit Bansal, and Yun-Nung Chen, editors, *Findings of the Association for Computational Linguistics: EMNLP 2024*, pages 3411–3425, Miami, Florida, USA, November 2024. Association for Computational Linguistics. doi: 10.18653/v1/2024.findings-emnlp.195.
- [19] Maritza Bustos-Lopez, Nicandro Cruz-Ramirez, Alejandro Guerra-Hernandez, Laura Nely Sánchez-Morales, Nancy Aracely Cruz-Ramos, and Giner Alor-Hernandez. Wearables for engagement detection in learning environments: A review. *Biosensors*, 12(7):509, 2022.
- [20] Sara Campanella, Ayham Altaieb, Alberto Belli, Paola Pierleoni, and Lorenzo Palma. A Method for Stress Detection Using Empatica E4 Bracelet and Machine-Learning Techniques. *Sensors*, 23(7):3565, January 2023. ISSN 1424-8220. doi: 10.3390/s23073565.

- [21] Marta Casanovas Ortega, Elisa Bruno, and Mark P. Richardson. Electrodermal activity response during seizures: A systematic review and meta-analysis. *Epilepsy & Behavior: E&B*, 134:108864, September 2022. ISSN 1525-5069. doi: 10.1016/j.yebeh.2022.108864.
- [22] Jierun Chen, Shiu-hong Kao, Hao He, Weipeng Zhuo, Song Wen, Chul-Ho Lee, and S.-H. Gary Chan. Run, Don't Walk: Chasing Higher FLOPS for Faster Neural Networks. In *2023 IEEE/CVF Conference on Computer Vision and Pattern Recognition (CVPR)*, pages 12021–12031, Vancouver, BC, Canada, June 2023. IEEE. ISBN 979-8-3503-0129-8. doi: 10.1109/CVPR52729.2023.01157.
- [23] Zhengyu Chen, Siqi Wang, Teng Xiao, Yudong Wang, Shiqi Chen, Xunliang Cai, Junxian He, and Jingang Wang. Revisiting Scaling Laws for Language Models: The Role of Data Quality and Training Strategies. In Wanxiang Che, Joyce Nabende, Ekaterina Shutova, and Mohammad Taher Pilehvar, editors, *Proceedings of the 63rd Annual Meeting of the Association for Computational Linguistics (Volume 1: Long Papers)*, pages 23881–23899, Vienna, Austria, July 2025. Association for Computational Linguistics. ISBN 979-8-89176-251-0. doi: 10.18653/v1/2025.acl-long.1163.
- [24] Davide Chicco and Giuseppe Jurman. The advantages of the Matthews correlation coefficient (MCC) over F1 score and accuracy in binary classification evaluation. *BMC Genomics*, 21(1):6, January 2020. ISSN 1471-2164. doi: 10.1186/s12864-019-6413-7.
- [25] Donna L. Coffman, Xizhen Cai, Runze Li, and Noelle R. Leonard. Challenges and Opportunities in Collecting and Modeling Ambulatory Electrodermal Activity Data. *JMIR biomedical engineering*, 5(1):e17106, 2020. ISSN 2561-3278. doi: 10.2196/17106.
- [26] Akbar Dehghani, Omid Sarbishei, Tristan Glatard, and Emad Shihab. A Quantitative Comparison of Overlapping and Non-Overlapping Sliding Windows for Human Activity Recognition Using Inertial Sensors. *Sensors*, 19(22):5026, January 2019. ISSN 1424-8220. doi: 10.3390/s19225026.
- [27] Janez Demšar. Statistical Comparisons of Classifiers over Multiple Data Sets. *J. Mach. Learn. Res.*, 7: 1–30, December 2006. ISSN 1532-4435.
- [28] Seyma Derdiyok, Fatma Patlar Akbulut, and Cagatay Catal. Neurophysiological and biosignal data for investigating occupational mental fatigue: MEFAR dataset. *Data in Brief*, 52:109896, February 2024. ISSN 2352-3409. doi: 10.1016/j.dib.2023.109896.
- [29] Elena Di Lascio, Shkurta Gashi, and Silvia Santini. Unobtrusive Assessment of Students' Emotional Engagement during Lectures Using Electrodermal Activity Sensors. *Proc. ACM Interact. Mob. Wearable Ubiquitous Technol.*, 2(3):103:1–103:21, September 2018. doi: 10.1145/3264913.
- [30] Elena Di Lascio, Shkurta Gashi, and Silvia Santini. Laughter Recognition Using Non-invasive Wearable Devices. In *Proceedings of the 13th EAI International Conference on Pervasive Computing Technologies for Healthcare, PervasiveHealth'19*, pages 262–271, New York, NY, USA, May 2019. Association for Computing Machinery. ISBN 978-1-4503-6126-2. doi: 10.1145/3329189.3329216.
- [31] Elena Di Lascio, Shkurta Gashi, Maike E. Debus, and Silvia Santini. Automatic Recognition of Flow During Work Activities Using Context and Physiological Signals. In *2021 9th International Conference on Affective Computing and Intelligent Interaction (ACII)*, pages 1–8, Nara, Japan, September 2021. IEEE. doi: 10.1109/ACII52823.2021.9597434.
- [32] Cheng Ding, Zhicheng Guo, Zhaoliang Chen, Randall J Lee, Cynthia Rudin, and Xiao Hu. SiamQuality: A ConvNet-based foundation model for photoplethysmography signals. *Physiological Measurement*, 45(8):085004, August 2024. ISSN 0967-3334. doi: 10.1088/1361-6579/ad6747.
- [33] Vipula Dissanayake, Sachith Seneviratne, Rajib Rana, Elliott Wen, Tharindu Kaluarachchi, and Suranga Nanayakkara. SigRep: Toward Robust Wearable Emotion Recognition With Contrastive Representation Learning. *IEEE Access*, 10:18105–18120, 2022. ISSN 2169-3536. doi: 10.1109/ACCESS.2022.3149509.
- [34] Alexey Dosovitskiy, Lucas Beyer, Alexander Kolesnikov, Dirk Weissenborn, Xiaohua Zhai, Thomas Unterthiner, Mostafa Dehghani, Matthias Minderer, Georg Heigold, Sylvain Gelly, Jakob Uszkoreit, and Neil Houlsby. An Image is Worth 16x16 Words: Transformers for Image Recognition at Scale. In *International Conference on Learning Representations*, Addis Ababa, Ethiopia, October 2020. International Conference on Learning Representations (ICLR).
- [35] Vasilii Feofanov, Songkang Wen, Marius Alonso, Romain Ilbert, Hongbo Guo, Malik Tiomoko, Lujia Pan, Jianfeng Zhang, and Ievgen Redko. Mantis: Lightweight Calibrated Foundation Model for User-Friendly Time Series Classification, February 2025.

- [36] Nan Gao, Wei Shao, Mohammad Saiedur Rahaman, and Flora D. Salim. N-Gage: Predicting in-class Emotional, Behavioural and Cognitive Engagement in the Wild. *Proc. ACM Interact. Mob. Wearable Ubiquitous Technol.*, 4(3):79:1–79:26, September 2020. doi: 10.1145/3411813.
- [37] Francisco M. Garcia-Moreno and Marta Badenes-Sastre. EmoPulse Moments E4 Dataset (EPM-E4): An Exhaustive Collection of Emotion-Related Data from Empatica E4 Wearable, September 2020.
- [38] Shkurta Gashi, Elena Di Lascio, and Silvia Santini. Using Unobtrusive Wearable Sensors to Measure the Physiological Synchrony Between Presenters and Audience Members. *Proc. ACM Interact. Mob. Wearable Ubiquitous Technol.*, 3(1):13:1–13:19, March 2019. doi: 10.1145/3314400.
- [39] Shkurta Gashi, Elena Di Lascio, Bianca Stancu, Vedant Das Swain, Varun Mishra, Martin Gjoreski, and Silvia Santini. Detection of Artifacts in Ambulatory Electrodermal Activity Data. *Proc. ACM Interact. Mob. Wearable Ubiquitous Technol.*, 4(2):44:1–44:31, June 2020. doi: 10.1145/3397316.
- [40] Shkurta Gashi, Lidia Alecci, Elena Di Lascio, Maike E. Debus, Francesca Gasparini, and Silvia Santini. The Role of Model Personalization for Sleep Stage and Sleep Quality Recognition Using Wearables. *IEEE Pervasive Computing*, 21(2):69–77, April 2022. ISSN 1558-2590. doi: 10.1109/MPRV.2022.3164334.
- [41] Shkurta Gashi, Chulhong Min, Alessandro Montanari, Silvia Santini, and Fahim Kawsar. A multidevice and multimodal dataset for human energy expenditure estimation using wearable devices. *Scientific Data*, 9(1):537, September 2022. ISSN 2052-4463. doi: 10.1038/s41597-022-01643-5.
- [42] Martin Gjoreski, Tine Kolenik, Timotej Knez, Mitja Luštrek, Matjaž Gams, Hristijan Gjoreski, and Veljko Pejović. Datasets for Cognitive Load Inference Using Wearable Sensors and Psychological Traits. *Applied Sciences*, 10(11):3843, January 2020. ISSN 2076-3417. doi: 10.3390/app10113843.
- [43] Mononito Goswami, Konrad Szafer, Arjun Choudhry, Yifu Cai, Shuo Li, and Artur Dubrawski. MO-MENT: A family of open time-series foundation models. In *Proceedings of the 41st International Conference on Machine Learning*, volume 235 of *ICML '24*, pages 16115–16152, Vienna, Austria, July 2024. JMLR.org.
- [44] Margherita Grandini, Enrico Bagli, and Giorgio Visani. Metrics for Multi-Class Classification: An Overview, August 2020.
- [45] Alberto Greco, Gaetano Valenza, Antonio Lanata, Enzo Pasquale Scilingo, and Luca Citi. cvxEDA: A Convex Optimization Approach to Electrodermal Activity Processing. *IEEE Transactions on Biomedical Engineering*, 63(4):797–804, April 2016. ISSN 1558-2531. doi: 10.1109/TBME.2015.2474131.
- [46] Md-Billal Hossain, Youngsun Kong, Hugo F. Posada-Quintero, and Ki H. Chon. Comparison of Electrodermal Activity from Multiple Body Locations Based on Standard EDA Indices’ Quality and Robustness against Motion Artifact. *Sensors*, 22(9):3177, January 2022. ISSN 1424-8220. doi: 10.3390/s22093177.
- [47] Md. Billal Hossain, Youngsun Kong, Hugo Posada-Quintero, and Ki Chon. *Electrodermal Activity: Applications and Challenges*, pages 475–496. Cambridge University Press, November 2024. ISBN 978-1-316-51855-7. doi: 10.1017/9781009000796.022.
- [48] Seyedmajid Hosseini, Raju Gottumukkala, Satya Katragadda, Ravi Teja Bhupatiraju, Ziad Ashkar, Christoph W. Borst, and Kenneth Cochran. A multimodal sensor dataset for continuous stress detection of nurses in a hospital. *Scientific Data*, 9(1):255, June 2022. ISSN 2052-4463. doi: 10.1038/s41597-022-01361-y.
- [49] Talha Iqbal, Andrew J. Simpkin, Davood Roshan, Nicola Glynn, John Killilea, Jane Walsh, Gerard Molloy, Sandra Ganly, Hannah Ryman, Eileen Coen, Adnan Elahi, William Wijns, and Atif Shahzad. Stress Monitoring Using Wearable Sensors: A Pilot Study and Stress-Predict Dataset. *Sensors*, 22(21):8135, January 2022. ISSN 1424-8220. doi: 10.3390/s22218135.
- [50] Alistair E. W. Johnson, Tom J. Pollard, Lu Shen, Li-wei H. Lehman, Mengling Feng, Mohammad Ghassemi, Benjamin Moody, Peter Szolovits, Leo Anthony Celi, and Roger G. Mark. MIMIC-III, a freely accessible critical care database. *Scientific Data*, 3(1):160035, May 2016. ISSN 2052-4463. doi: 10.1038/sdata.2016.35.
- [51] Alistair E. W. Johnson, Lucas Bulgarelli, Lu Shen, Alvin Gayles, Ayad Shammout, Steven Horng, Tom J. Pollard, Sicheng Hao, Benjamin Moody, Brian Gow, Li-wei H. Lehman, Leo A. Celi, and Roger G. Mark. MIMIC-IV, a freely accessible electronic health record dataset. *Scientific Data*, 10(1):1, January 2023. ISSN 2052-4463. doi: 10.1038/s41597-022-01899-x.
- [52] Daniel Kahneman, Bernard Tursky, David Shapiro, and Andrew Crider. Pupillary, heart rate, and skin resistance changes during a mental task. *Journal of experimental psychology*, 79(1p1):164, 1969.

- [53] Diederik P. Kingma and Jimmy Ba. Adam: A Method for Stochastic Optimization, 2017.
- [54] Zuzana Koscova, Valdery Moura Junior, Matthew Reyna, Shenda Hong, Aditya Gupta, Manohar Ghanta, Reza Sameni, Aaron Aguirre, Qiao Li, Sahar Zafar, Gari Clifford, and M Brandon Westover. Harvard-Emory ECG Database, 2025.
- [55] Matias Laporte, Martin Gjoreski, and Marc Langheinrich. LAUREATE: A Dataset for Supporting Research in Affective Computing and Human Memory Augmentation. *Proc. ACM Interact. Mob. Wearable Ubiquitous Technol.*, 7(3):106:1–106:41, September 2023. doi: 10.1145/3610892.
- [56] Phuc H. Le-Khac, Graham Healy, and Alan F. Smeaton. Contrastive Representation Learning: A Framework and Review. *IEEE Access*, 8:193907–193934, 2020. ISSN 2169-3536. doi: 10.1109/ACCESS.2020.3031549.
- [57] Hyung-Chul Lee, Yoonsang Park, Soo Bin Yoon, Seong Mi Yang, Dongnyeok Park, and Chul-Woo Jung. VitalDB, a high-fidelity multi-parameter vital signs database in surgical patients. *Scientific Data*, 9(1): 279, June 2022. ISSN 2052-4463. doi: 10.1038/s41597-022-01411-5.
- [58] Simon Lee and Kai Akamatsu. Foundation Models for Physiological Signals: Opportunities and Challenges, August 2025.
- [59] Jun Li, Aaron D. Aguirre, Valdery Moura, Jiarui Jin, Che Liu, Lanhai Zhong, Chenxi Sun, Gari Clifford, M. Brandon Westover, and Shenda Hong. An Electrocardiogram Foundation Model Built on over 10 Million Recordings. *Nejm Ai*, 2(7):A10a2401033, July 2025. ISSN 2836-9386. doi: 10.1056/aioa2401033.
- [60] Yu Liu, María-Itatí Palacio, Taha Bikki, Cesar Toledo, Yu Ouyang, Zhongzheng Li, Zhengyi Wang, Francisco Toledo, Hong Zeng, and María-Trinidad Herrero. Machine Learning, Physiological Signals, and Emotional Stress/Anxiety: Pitfalls and Challenges. *Applied Sciences*, 15(21):11777, January 2025. ISSN 2076-3417. doi: 10.3390/app152111777.
- [61] Junoš Lukan, Martin Gjoreski, Heidi Mauersberger, Annekatrin Hoppe, Ursula Hess, and Mitja Luštrek. Analysing Physiology of Interpersonal Conflicts Using a Wrist Device. In Achilles Kameas and Kostas Stathis, editors, *Ambient Intelligence*, pages 162–167, Cham, 2018. Springer International Publishing. ISBN 978-3-030-03062-9. doi: 10.1007/978-3-030-03062-9_13.
- [62] Yunfei Luo, Yuliang Chen, Asif Salekin, and Tauhidur Rahman. Toward Foundation Model for Multivariate Wearable Sensing of Physiological Signals, May 2025.
- [63] Erika Lutin, Ryuga Hashimoto, Walter De Raedt, and Chris Van Hoof. Feature Extraction for Stress Detection in Electrodermal Activity:. In *Proceedings of the 14th International Joint Conference on Biomedical Engineering Systems and Technologies*, pages 177–185, Online Streaming, — Select a Country —, 2021. SCITEPRESS - Science and Technology Publications. ISBN 978-989-758-490-9. doi: 10.5220/0010244601770185.
- [64] Katie Matton, Robert Lewis, John Guttag, and Rosalind Picard. Contrastive Learning of Electrodermal Activity Representations for Stress Detection. In *Proceedings of the Conference on Health, Inference, and Learning*, pages 410–426, Cambridge, MA, USA, June 2023. PMLR.
- [65] Daniel McDuff, Seamus Thomson, Samy Abdel-Ghaffar, Isaac R. Galatzer-Levy, Ming-Zher Poh, Jake Sunshine, Andrew Barakat, Conor Heneghan, and Lindsey Sunden. What Does Large-scale Electrodermal Sensing Reveal?, February 2024.
- [66] Kaden McKeen, Sameer Masood, Augustin Toma, Barry Rubin, and Bo Wang. ECG-FM: An open electrocardiogram foundation model. *JAMIA open*, 8(5):ooaf122, October 2025. ISSN 2574-2531. doi: 10.1093/jamiaopen/ooaf122.
- [67] Varun Mishra, Sougata Sen, Grace Chen, Tian Hao, Jeffrey Rogers, Ching-Hua Chen, and David Kotz. Evaluating the Reproducibility of Physiological Stress Detection Models. *Proc. ACM Interact. Mob. Wearable Ubiquitous Technol.*, 4(4):147:1–147:29, December 2020. doi: 10.1145/3432220.
- [68] Girish Narayanswamy, Xin Liu, Kumar Ayush, Yuzhe Yang, Xuhai Xu, Shun Liao, Jake Garrison, Shyam Tailor, Jake Sunshine, Yun Liu, Tim Althoff, Shrikanth Narayanan, Pushmeet Kohli, Jiening Zhan, Mark Malhotra, Shwetak Patel, Samy Abdel-Ghaffar, and Daniel McDuff. Scaling Wearable Foundation Models, October 2024.
- [69] Sameer Neupane, Mithun Saha, Nasir Ali, Timothy Hnat, Shahin Alan Samiei, Anandathirtha Nandugudi, David M. Almeida, and Santosh Kumar. Momentary Stressor Logging and Reflective Visualizations: Implications for Stress Management with Wearables. In *Proceedings of the 2024 CHI Conference on Human Factors in Computing Systems*, CHI '24, pages 1–19, New York, NY, USA, May 2024. Association for Computing Machinery. ISBN 979-8-4007-0330-0. doi: 10.1145/3613904.3642662.

- [70] Michael Owusu-Adjei, James Ben Hayfron-Acquah, Twum Frimpong, and Gaddafi Abdul-Salaam. Imbalanced class distribution and performance evaluation metrics: A systematic review of prediction accuracy for determining model performance in healthcare systems. *PLOS Digital Health*, 2(11):e0000290, November 2023. ISSN 2767-3170. doi: 10.1371/journal.pdig.0000290.
- [71] Adam Paszke, Sam Gross, Francisco Massa, Adam Lerer, James Bradbury, Gregory Chanan, Trevor Killeen, Zeming Lin, Natalia Gimelshein, Luca Antiga, Alban Desmaison, Andreas Köpf, Edward Yang, Zach DeVito, Martin Raison, Alykhan Tejani, Sasank Chilamkurthy, Benoit Steiner, Lu Fang, Junjie Bai, and Soumith Chintala. *PyTorch: An Imperative Style, High-Performance Deep Learning Library*, pages 8026–8037. Curran Associates Inc., Red Hook, NY, USA, 2019.
- [72] Arvind Pillai, Dimitris Spathis, Fahim Kawsar, and Mohammad Malekzadeh. PaPaGei: Open Foundation Models for Optical Physiological Signals, February 2025.
- [73] Anuja Pinge, Vinaya Gad, Dheryta Jaisighani, Surjya Ghosh, and Sougata Sen. Detection and monitoring of stress using wearables: a systematic review. *Frontiers in Computer Science*, 6:1478851, 2024.
- [74] Ming-Zher Poh, Tobias Loddenkemper, Claus Reinsberger, Nicholas C. Swenson, Shubhi Goyal, Mangwe C. Sabtala, Joseph R. Madsen, and Rosalind W. Picard. Convulsive seizure detection using a wrist-worn electrodermal activity and accelerometry biosensor. *Epilepsia*, 53(5):e93–97, May 2012. ISSN 1528-1167. doi: 10.1111/j.1528-1167.2012.03444.x.
- [75] Md. Rafiul Amin, Dilranjan S. Wickramasuriya, and Rose T. Faghieh. A Wearable Exam Stress Dataset for Predicting Grades using Physiological Signals. In *2022 IEEE Healthcare Innovations and Point of Care Technologies (HI-POCT)*, pages 30–36, Houston, TX, USA, March 2022. IEEE. doi: 10.1109/HI-POCT54491.2022.9744065.
- [76] Saeed Ur Rehman, Anwar Ali, Adil Mehmood Khan, and Cynthia Okpala. Human Activity Recognition: A Comparative Study of Validation Methods and Impact of Feature Extraction in Wearable Sensors. *Algorithms*, 17(12):556, December 2024. ISSN 1999-4893. doi: 10.3390/a17120556.
- [77] Attila Reiss, Ina Indlekofer, Philip Schmidt, and Kristof Van Laerhoven. Deep PPG: Large-Scale Heart Rate Estimation with Convolutional Neural Networks. *Sensors*, 19(14):3079, January 2019. ISSN 1424-8220. doi: 10.3390/s19143079.
- [78] Matthew A Reyna, Nadi Sadr, Erick A Perez Alday, Annie Gu, Amit J Shah, Chad Robichaux, Ali Bahrami Rad, Andoni Elola, Salman Seyedi, Sardar Ansari, Hamid Ghanbari, Qiao Li, Ashish Sharma, and Gari D Clifford. Will Two Do? Varying Dimensions in Electrocardiography: The PhysioNet/Computing in Cardiology Challenge 2021. In *2021 Computing in Cardiology (CinC)*, volume 48, pages 1–4, Brno, Czech Republic, September 2021. IEEE. doi: 10.23919/CinC53138.2021.9662687.
- [79] William L Romine, Noah L Schroeder, Josephine Graft, Fan Yang, Reza Sadeghi, Mahdiah Zabihi-mayvan, Dipesh Kadariya, and Tanvi Banerjee. Using machine learning to train a wearable device for measuring students cognitive load during problem-solving activities based on electrodermal activity, body temperature, and heart rate: Development of a cognitive load tracker for both personal and classroom use. *Sensors*, 20(17):4833, 2020.
- [80] Aaqib Saeed, Flora D. Salim, Tanir Ozcelebi, and Johan Lukkien. Federated Self-Supervised Learning of Multisensor Representations for Embedded Intelligence. *IEEE Internet of Things Journal*, 8(2): 1030–1040, January 2021. ISSN 2327-4662. doi: 10.1109/JIOT.2020.3009358.
- [81] Mithun Saha, Maxwell A. Xu, Wanting Mao, Sameer Neupane, James M. Rehg, and Santosh Kumar. Pulse-PPG: An Open-Source Field-Trained PPG Foundation Model for Wearable Applications across Lab and Field Settings. *Proc. ACM Interact. Mob. Wearable Ubiquitous Technol.*, 9(3):126:1–126:35, September 2025. doi: 10.1145/3749494.
- [82] Philip Schmidt, Attila Reiss, Robert Duerichen, Claus Marberger, and Kristof Van Laerhoven. Introducing WESAD, a Multimodal Dataset for Wearable Stress and Affect Detection. In *Proceedings of the 20th ACM International Conference on Multimodal Interaction, ICMI '18*, pages 400–408, New York, NY, USA, October 2018. Association for Computing Machinery. ISBN 978-1-4503-5692-3. doi: 10.1145/3242969.3242985.
- [83] Christopher Slade, Yinan Sun, Wei Cheng Chao, Chih-Chun Chen, Roberto M. Benzo, and Peter Washington. Current challenges and opportunities in active and passive data collection for mobile health sensing: A scoping review. *JAMIA open*, 8(4):oaf025, August 2025. ISSN 2574-2531. doi: 10.1093/jamiaopen/oaaf025.

- [84] Jamiyan Sukhbaatar, Satoshi Imamura, Ibuki Inoue, Shoya Murakami, Kazi Mahmudul Hassan, Seungwoo Han, Ingon Chanpornpakdi, and Toshihisa Tanaka. SingLEM: Single-Channel Large EEG Model, September 2025.
- [85] Henrik Svoren, Vajira Thambawita, Pål Halvorsen, Petter Jakobsen, Enrique Garcia-Ceja, Farzan Ma-jeed Noori, Hugo L. Hammer, Mathias Lux, Michael Alexander Riegler, and Steven Alexander Hicks. Toadstool: A dataset for training emotional intelligent machines playing Super Mario Bros. In *Proceedings of the 11th ACM Multimedia Systems Conference, MMSys '20*, pages 309–314, New York, NY, USA, May 2020. Association for Computing Machinery. ISBN 978-1-4503-6845-2. doi: 10.1145/3339825.3394939.
- [86] Mingxing Tan and Quoc Le. Efficientnet: Rethinking model scaling for convolutional neural networks. In *International conference on machine learning*, pages 6105–6114, Long Beach, CA, USA, 2019. PMLR, PMLR.
- [87] Andrés Tello, Victoria Degeler, and Alexander Lazovik. Too good to be true: Accuracy overestimation in (re) current practices for human activity recognition. In *2024 IEEE International Conference on Pervasive Computing and Communications Workshops and Other Affiliated Events (PerCom Workshops)*, pages 511–517, Biarritz, France, 2024. IEEE.
- [88] James Truslow, Angela Spillane, Huiming Lin, Katherine Cyr, Adeeti Ullal, Edith Arnold, Ron Huang, Laura Rhodes, Jennifer Block, Jamie Stark, James Kretlow, Alexis L. Beatty, Andreas Werdich, Deepali Bankar, Matt Bianchi, Ian Shapiro, Jaime Villalpando, Sharon Ravindran, Irida Mance, Adam Phillips, John Earl, Rahul C. Deo, Sumbul A. Desai, and Calum A. MacRae. Understanding activity and physiology at scale: The Apple Heart & Movement Study. *npj Digital Medicine*, 7(1):242, September 2024. ISSN 2398-6352. doi: 10.1038/s41746-024-01187-5.
- [89] Aaron van den Oord, Yazhe Li, and Oriol Vinyals. Representation Learning with Contrastive Predictive Coding, January 2019.
- [90] Yedukondala Rao Veeranki, Nagarajan Ganapathy, Ramakrishnan Swaminathan, and Hugo F. Posada-Quintero. Comparison of Electrodermal Activity Signal Decomposition Techniques for Emotion Recognition. *IEEE Access*, 12:19952–19966, 2024. ISSN 2169-3536. doi: 10.1109/ACCESS.2024.3361832.
- [91] Miguel Viana-Matesanz and Carmen Sánchez-Ávila. Adaptive Normalization and Feature Extraction for Electrodermal Activity Analysis. *Mathematics*, 12(2):202, January 2024. ISSN 2227-7390. doi: 10.3390/math12020202.
- [92] Ke Wang, Jiamu Yang, Ayush Shetty, and Jessilyn Dunn. DREAMT: Dataset for Real-time sleep stage EstimAtion using Multisensor wearable Technology, 2024.
- [93] Rongjie Yi, Ting Cao, Ao Zhou, Xiao Ma, Shangguang Wang, and Mengwei Xu. Boosting DNN Cold Inference on Edge Devices. In *Proceedings of the 21st Annual International Conference on Mobile Systems, Applications and Services, MobiSys '23*, pages 516–529, New York, NY, USA, June 2023. Association for Computing Machinery. ISBN 979-8-4007-0110-8. doi: 10.1145/3581791.3596842.
- [94] Guo-Qiang Zhang, Licong Cui, Remo Mueller, Shiqiang Tao, Matthew Kim, Michael Rueschman, Sara Mariani, Daniel Mobley, and Susan Redline. The National Sleep Research Resource: Towards a sleep data commons. *Journal of the American Medical Informatics Association*, 25(10):1351–1358, October 2018. ISSN 1527-974X. doi: 10.1093/jamia/ocy064.
- [95] Yuwei Zhang, Kumar Ayush, Siyuan Qiao, A. Ali Heydari, Girish Narayanswamy, Maxwell A. Xu, Ahmed A. Metwally, Shawn Xu, Jake Garrison, Xuhai Xu, Tim Althoff, Yun Liu, Pushmeet Kohli, Jiening Zhan, Mark Malhotra, Shwetak Patel, Cecilia Mascolo, Xin Liu, Daniel McDuff, and Yuzhe Yang. SensorLM: Learning the Language of Wearable Sensors, June 2025.

Table A.1: Summary of datasets with their corresponding data-sharing agreements. This table includes all datasets, including citations and the "Reshareable" column, for inclusion in the appendix.

Dataset Name	License
BiHeartS [3]	✓- data share agreement
BIG IDEAS [11]	✓- with original license (ODC-BY 1)
Dynamics in the workplace [61]	✓- data share agreement
EmpaticaE4Stress [20]	✓- (CCBY 4) with original license
EPM-E4 [37]	✓- (CCBY 4) with original license
LAUREATE [55]	✓- data share agreement
MEFAR [28]	✓- (CCBY 4) with original license
M2Sleep [40]	✓- data share agreement
PPG-Dalia [77]	✓- (CCBY 4) with original license
SEED [29]	✓- data share agreement
SEED-II-Lab [29]	✓- data share agreement
SEED-II-Wild [29]	✓- data share agreement
Stress Predict [49]	✓- (MIT) with original license
ToadStool [85]	✓- (CCBY 4) with original license
WEEE [41]	✓- (CCBY 4) with original license
WESD [75]	✓- with original license (ODC-BY 1)
Workplace [31]	✓- data share agreement
APSync [38]	✓- data share agreement
HeartS [2]	✓- data share agreement
USILaughS [30]	✓- data share agreement
WESAD [82]	✓- (CCBY 4) with original license
Nurses' Stress [48]	✓- (ODbL 1) with original license
DREAMT [92]	✗- PhysioNet Restricted Health Data Use Agreement 1.5.0
HHISS [42]	✗- no license specified

A Methodology, Evaluation, Transparency, and Availability (META) Appendix

A.1 Additional dataset information

We report in Table A.1 information about the original license associated with the datasets making up the EDAMAME collection. The datasets that we re-share are all under their original license, if so required. For the datasets that require a data sharing agreement to be signed, we contacted the original authors, which all agreed to for re-sharing under the conditions in the original data sharing agreement.

A.2 Baseline feature sets

In section 5.1 we explain how we use two handcrafted feature sets as baseline to evaluate the embeddings from our UME foundation model. The first feature set, which we call *generic handcrafted feature set*, consists of four statistics, i.e., mean, minimum, maximum and standard deviation, computed for both the phasic and tonic EDA components, as well as the original non-decomposed EDA signal. This feature set emulates baseline used by related work to evaluate foundation models for physiological data [1, 72]. The second set of features, which we call *EDA-specific handcrafted feature set*, is a broader set of features commonly used in EDA classification pipelines [4, 39]. In addition to the generic statistics, this set incorporates signal dynamics (e.g., slopes and derivatives), morphological peak characteristics, and frequency-domain components. This set consists of 15 base features, resulting in a total of 45 features per window (15 features \times 3 EDA components).

Table A.3 details the exact mathematical formulations for all 15 base features and specifies their inclusion in the respective baseline sets.

We report in Table A.2 the feature size of the feature extraction methods used in this work.

Table A.2: Overview of the models and feature sets used in the experimental evaluation. We report the model size (number of trainable parameters) and the dimensionality of the feature space (d) used for linear probing.

Model / Feature Set	Model Size	Feature Dim. (d)
Handcrafted Methods		
Generic HC	N/A	12
EDA-specific HC	N/A	45
Generalist Foundation Models		
Mantis [35]	~ 8 M	768
Chronos [8]	~ 200 M	1536
MOMENT [43]	~ 385 M	1024
Ours		
UME	~ 1 M	64

A.3 Hyperparameter grid for the logistic regression

In Table A.4 we report the hyperparameter grid we used with the logistic regression. We used a 3-fold inner cross-validation to search for the best configuration of hyperparameter during our feature evaluation through linear probing.

A.4 Training details

We train the UME foundation model using the Adam optimizer [53] (learning rate 0.001 and weight decay 0.01). We also use a learning rate scheduler, Reduce On Plateau (factor 0.5), to decrease the learning rate during training. We train the model for a maximum of 400 epochs, with early stopping, with a batch size of 512. In total, we train our model for approximately 5 days, using an Nvidia A6000 GPU¹⁴. We implement the foundation model in Python, using the Pytorch [71] and Pytorch-Lightning libraries.

A.5 Data augmentations for EDA data

We report in Table A.5 the list of data augmentations used to train our UME foundation model with contrastive learning. We use the same set proposed by Matton et al. [64], which contains EDA-specific augmentations.

¹⁴<https://www.nvidia.com/en-us/products/workstations/rtx-a6000/>

Table A.3: Mathematical formulations for the 15 base hand-crafted features extracted from EDA time series signals (x) of length N . All features are computed independently for the tonic, phasic, and original EDA components. The "Feature Set(s)" column indicates whether the feature was used in the Generic baseline (12 total features) or the EDA-specific baseline (45 total features).

Feature	Mathematical Notation or Formula	Feature Set(s)
Time-domain		
Mean	$\frac{1}{N} \sum_{i=1}^N x_i$	Generic & EDA-specific
Minimum	$\min(x_1, x_2, \dots, x_N)$	Generic & EDA-specific
Maximum	$\max(x_1, x_2, \dots, x_N)$	Generic & EDA-specific
Standard Deviation	$\sqrt{\frac{1}{N-1} \sum_{i=1}^N (x_i - \bar{x})^2}$	Generic & EDA-specific
Dynamic Range	$\max(x_1, x_2, \dots, x_N) - \min(x_1, x_2, \dots, x_N)$	EDA-specific only
Slope	$\frac{x_N - x_1}{N-1}$	EDA-specific only
Absolute Value of Slope	$\left \frac{x_N - x_1}{N-1} \right $	EDA-specific only
Mean of the First Derivative	$\frac{1}{N-1} \sum_{i=1}^{N-1} (x_{i+1} - x_i)$	EDA-specific only
Std. Dev. of the First Derivative	$\sqrt{\frac{1}{N-2} \sum_{i=1}^{N-1} ((x_{i+1} - x_i) - \bar{x}')^2}$	EDA-specific only
Number of EDA Peaks	Count of local maxima in the window	EDA-specific only
Amplitude of EDA Peaks	Mean amplitude of local maxima in the window	EDA-specific only
Frequency Domain (Fast Fourier Transform)		
Direct Current (DC)	X_0	EDA-specific only
Sum of Frequency Coefficients	$\sum_{k=1}^N X_k $	EDA-specific only
Information Entropy	$-\sum_{k=1}^N P(X_k) \log_2(P(X_k))$	EDA-specific only
Spectral Energy	$\sum_{k=1}^N X_k ^2$	EDA-specific only

Table A.4: Hyperparameter Grid for Logistic Regression

Hyperparameter	Values
Regularization strength (C)	0.01, 0.1, 1, 10
Solver	lbfgs, liblinear
Penalty	L2
Max iterations	10000
Class weight	balanced

Table A.5: Summary of Electrodermal Activity (EDA) Data Augmentations used to train the UME foundation model. The table details both EDA-specific transforms designed to isolate physiological components or simulate artifacts, and generic time series transforms. The set is the same proposed by Matton et al. [64].

Augmentation	Type	Description	Parameter Range
Frequency Domain & Component Isolation			
Low-Pass Filter	EDA-Specific	Extracts tonic component; removes high-freq noise.	Cutoff $f \in [0.25, 1.0]$ Hz
High-Pass Filter	EDA-Specific	Extracts phasic component; removes slow drifts.	Cutoff $f \in [0.05, 0.25]$ Hz
Band-Pass Filter	EDA-Specific	Isolates information-rich EDA frequency bands.	Pass $f \in [0.05, 0.25]$ Hz
Band-Stop Filter	EDA-Specific	Rejects specific frequency bands.	Reject $f \in [0.75, 1.0]$ Hz
High Freq. Noise	EDA-Specific	Adds Gaussian noise only to frequencies > 1 Hz.	Noise $\sigma \in [0, 0.5]$
Artifact Simulation			
Jump Artifact	EDA-Specific	Simulates abrupt sensor movement/displacement.	Jump $\in [0.01, 0.2]\mu S$
Loose Sensor	EDA-Specific	Simulates electrode contact loss (signal drop).	Duration $t \in [5, 20]$ s
Thermoregulation Simulation			
Tonic Const. Scale	EDA-Specific	Scales tonic component (simulates constant temp).	Factor $s \in [0.25, 2]$
Tonic Amp. Warp	EDA-Specific	Time-varying scale of tonic component (changing conditions).	Spline $\sigma \in [0.01, 0.05]$
Generic Time Series			
Amp. Const. Scale	Generic	Applies constant scaling factor to the raw signal.	Factor $s \in [0.25, 2]$
Amplitude Warp	Generic	Applies smooth, time-varying scaling to raw signal.	Spline $\sigma \in [0.01, 0.05]$
Gaussian Noise	Generic	Adds random Gaussian noise to the raw signal.	$\sigma \in [0, 0.5]$
Time Shift	Generic	Shifts the signal window forward or backward.	Shift $t \in [5, 45]$ s
Temporal Cutout	Generic	Masks/zeros out a random sub-window of the signal.	Cutout $t \in [5, 15]$ s
Time Warp	Generic	Perturbs temporal dimension (local stretch/compress).	Spline $\sigma \in [0.01, 0.1]$
Permutation	Generic	Slices signal and randomly reorders sub-windows.	Segments $n \in [2, 6]$
Signal Flip	Generic	Inverts the signal over its amplitude dimension.	N/A

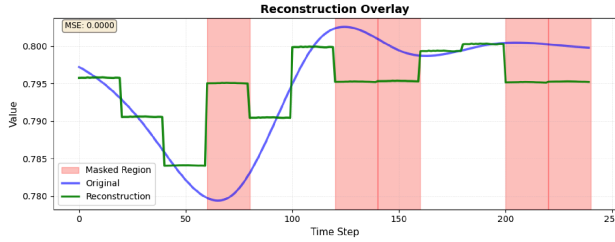


Figure B.1: Example of EDA signal reconstruction using MAE.

B Sensitivity & additional model studies

We perform sensitivity and additional studies to find the configuration of our UME foundation model. In this section, we report details for: implementation of an additional NN architecture, i.e., a Masked Autoencoder (MAE); studies on model size and hyperparameters for the EfficientNet architecture chosen for the UME foundation model, trained using contrastive learning.

We perform all training in this section using a subset (about 15% of the total data) of the train part of the EDAMAME collection of datasets. We do this to speed-up experimentation since, as reported in subsection 4.3, the complete model training takes about 5 days in total with a single A6000 NVIDIA GPU, due to the large scale of the train set.

B.1 Experiments with Masked Autoencoders (MAEs)

We train a reconstructive-based masked autoencoder (MAE), based on vision transformer (ViT) [34]. Narayanswamy et al. [68] also used a masked-autoencoder to train a foundation model for physiological data. We train the model using the following loss: let $\mathbf{x} \in \mathbb{R}^{T \times C}$ denote the input EDA signal, partitioned into N non-overlapping patches of size P , and let $\hat{\mathbf{x}}_i$ and \mathbf{x}_i denote the reconstructed and original i -th patch, respectively. Given a binary mask $\mathbf{m} \in \{0, 1\}^N$, where $m_i = 1$ indicates a masked patch and $m_i = 0$ a visible one, the reconstruction loss is defined as

$$\mathcal{L} = \alpha \mathcal{L}_{\text{masked}} + (1 - \alpha) \mathcal{L}_{\text{visible}}, \quad (2)$$

with

$$\mathcal{L}_{\text{masked}} = \frac{1}{\sum_i m_i} \sum_{i=1}^N m_i \ell(\hat{\mathbf{x}}_i, \mathbf{x}_i), \quad (3)$$

$$\mathcal{L}_{\text{visible}} = \frac{1}{\sum_i (1 - m_i)} \sum_{i=1}^N (1 - m_i) \ell(\hat{\mathbf{x}}_i, \mathbf{x}_i), \quad (4)$$

where $\ell(\cdot, \cdot)$ denotes either the mean absolute error (MAE) computed within each patch, and $\alpha \in [0, 1]$ controls the relative importance of masked versus visible patch reconstruction.

We experiment with the following configurations: $m \in \{0, 0.1, 0.4\}$ and $\alpha \in \{0.1, 0.5\}$. In Figure B.2 we report the validation loss during training curve for the configurations tested, and in Figure B.1 we show an example of a signal reconstruction at train end, over a validation sample. We also perform downstream evaluation on the BiHeartS dataset: however, no configuration leads to performance, in terms of balanced accuracy, above that of the Dummy classifier.

Given these findings, we believe that masked autoencoders are not optimal for the specific EDA data present in the EDAMAME collection of datasets.

B.2 EfficientNet ablation studies

We adopt an EfficientNet architecture for our UME foundation model, which we train using contrastive learning on EDA data. We perform ablation studies using different configurations of hyperparameters, which affect the model size. We compare the performance of the different models with respect to two criteria: validation loss and performance on a selected set of downstream tasks. We leave about 10% of the



Figure B.2: Validation loss during training for different configurations of masking and masking weight.

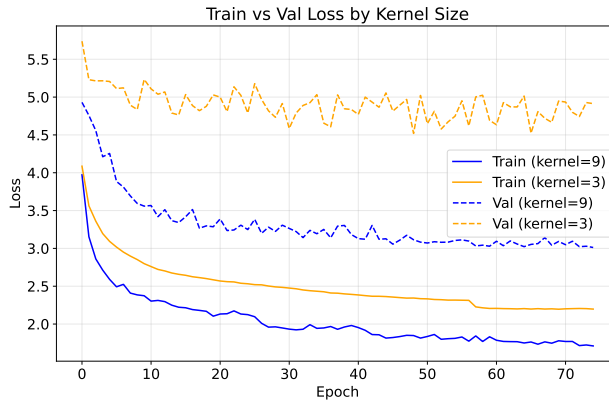


Figure B.3:

train dataset for validation during training, to also stop the training using early stopping (patience set to 30). We acknowledge that this selection may introduce bias in reporting the final results.

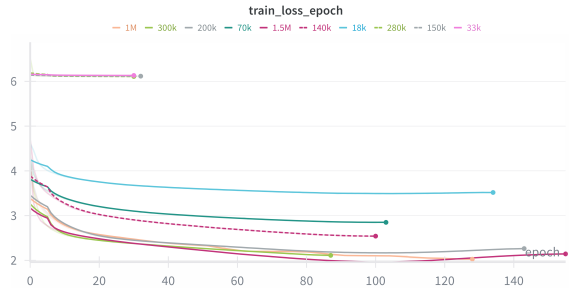
We do not select all possible hyperparameters. In particular, we set as fixed the following: loss temperature $\tau = 0.1$ (see loss definition in Equation 1); weights dropout at 50%.

We perform the hyperparameter selection through multiple experiments. We list the experiments in order of which we perform them.

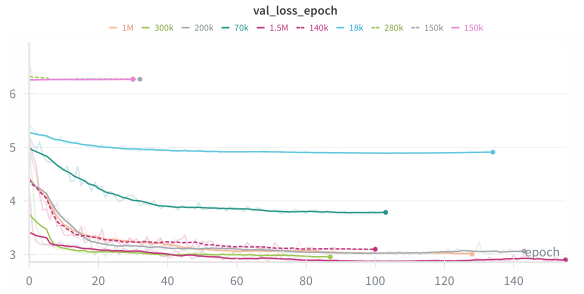
Kernel size We compare the following kernel sizes: 9 and 3. We choose 9 since the reaction time associated with EDA changes in approximately 2 seconds (9 samples with a sampling rate of 4 Hz is about 2.25 s) [15]; we choose 3 since the minimum rise time of an EDA signal is between 0.25s and 0.5 s [39].

We report in Figure B.3 the train and validation loss. We notice how the loss depends on the set in which it is computed, hence it cannot be directly compared between train and validation; however, given the same set and two models, the comparison can be performed, since we made sure to use the same splits for all experiments. Given these results, we select a kernel size of 3.

Model size The second set of experiments are related to the model size. In order to determine the size of the model, we modify the following hyperparameters: the stem channels [64, 32], the number of convolutional channels [8, 16, 32, 64, 92], the total number of convolutional blocks [2, 4, 8, 12, 16]; the head channels [32, 64]; and the final embeddings dimensionality [32, 64].



(a) Train loss for different model sizes



(b) Validation loss for different model sizes

We report the train and val losses in Figure B.4a and Figure B.4b respectively. From the comparison between the train and val losses, we conclude that there is an impact, in learning representation, from the model size. However, after about 1M parameters, the validation loss remains similar.

We select a model with about 1M parameters for our final training. The model contains the following parameters:

- stem channels: 64
- mbconv channels: 64
- num mbconv blocks: 16
- head channels: 248
- embedding dim: 64
- kernel size: 9

Table C.1: CPU Performance Comparison of Extractors

Extractor	CPU Time (mean) [ms]	CPU Time (SE) [ms]
MOMENT (128M)	4823.53	161.11
Chronos (28M)	721.34	28.91
Mantis (8M)	350.23	39.06
UME (1M)	184.56	3.12
EDA-specific hc	35.39	1.40
generic hc	0.09	0.01

C Additional results

Computational analysis complexity We report in Table C.1 the detailed performance metrics for the computation complexity analysis. This table mirrors the results in Figure 6.

Complete results for the downstream evaluation We report in Table C.2 and Table C.3 the complete results for our experimental evaluation. Specifically, we report the results in terms of balanced accuracy, Matthew’s Correlation Coefficient (MCC) [24] and F1-score. We report the results for both validation methods used, i.e., LOPO and TA cross-validations. Results are reported for all tasks in both validation methods. For the TA cross-validation, we do not report the results for *cognitive-load/relaxation* classification on the USILaughs dataset [30], since there was not enough data for each user to perform the temporal split.

Table C.2: Results of binary classification experiments, using the Leave One Participant Out (LOPO) cross-validation. Results shown as **metric \pm standard error**.

Dataset	Binary Task	Model	Metrics		
			Balanced Acc.	MCC	F1
Dreamt	Deep Sleep/REM	Dummy	0.73 \pm 0.05	-0.01 \pm 0.01	0.16 \pm 0.06
		Gen. HC	0.64 \pm 0.07	0.00 \pm 0.03	0.10 \pm 0.06
		EDA-spec. HC	0.54 \pm 0.05	0.02 \pm 0.03	0.19 \pm 0.07
		Mantis	0.59 \pm 0.05	0.02 \pm 0.04	0.18 \pm 0.07
		MOMENT	0.64 \pm 0.03	0.06 \pm 0.03	0.21 \pm 0.07
		Chronos	0.64 \pm 0.04	0.03 \pm 0.03	0.19 \pm 0.07
		UME	0.56 \pm 0.05	0.04 \pm 0.04	0.17 \pm 0.06
Dreamt	Sleep/Wake	Dummy	0.50 \pm 0.00	0.00 \pm 0.00	0.49 \pm 0.01
		Gen. HC	0.70 \pm 0.03	0.40 \pm 0.05	0.68 \pm 0.04
		EDA-spec. HC	0.74 \pm 0.02	0.48 \pm 0.04	0.72 \pm 0.03
		Mantis	0.77 \pm 0.02	0.52 \pm 0.04	0.74 \pm 0.03
		MOMENT	0.72 \pm 0.02	0.44 \pm 0.03	0.71 \pm 0.03
		Chronos	0.78 \pm 0.02	0.55 \pm 0.03	0.75 \pm 0.03
		UME	0.75 \pm 0.02	0.50 \pm 0.04	0.73 \pm 0.03
HHISS	Stress/calm	Dummy	0.50 \pm 0.00	-0.00 \pm 0.01	0.24 \pm 0.03
		Gen. HC	0.56 \pm 0.03	0.12 \pm 0.07	0.44 \pm 0.06
		EDA-spec. HC	0.64 \pm 0.03	0.28 \pm 0.07	0.55 \pm 0.04
		Mantis	0.63 \pm 0.03	0.26 \pm 0.06	0.53 \pm 0.04
		MOMENT	0.55 \pm 0.02	0.09 \pm 0.05	0.44 \pm 0.03
		Chronos	0.59 \pm 0.03	0.17 \pm 0.06	0.48 \pm 0.04
		UME	0.59 \pm 0.03	0.19 \pm 0.06	0.49 \pm 0.05
HeartS	Sleep/Wake	Dummy	0.50 \pm 0.00	0.00 \pm 0.00	0.08 \pm 0.02
		Gen. HC	0.66 \pm 0.09	0.28 \pm 0.16	0.32 \pm 0.11
		EDA-spec. HC	0.70 \pm 0.05	0.32 \pm 0.13	0.36 \pm 0.11
		Mantis	0.74 \pm 0.06	0.37 \pm 0.14	0.41 \pm 0.13
		MOMENT	0.70 \pm 0.04	0.27 \pm 0.06	0.33 \pm 0.09
		Chronos	0.73 \pm 0.06	0.34 \pm 0.11	0.39 \pm 0.12
		UME	0.71 \pm 0.06	0.30 \pm 0.10	0.35 \pm 0.10
WESAD	Low/High Arousal	Dummy	0.58 \pm 0.05	-0.02 \pm 0.03	0.05 \pm 0.03
		Gen. HC	0.61 \pm 0.09	0.10 \pm 0.14	0.26 \pm 0.13
		EDA-spec. HC	0.63 \pm 0.08	0.13 \pm 0.11	0.33 \pm 0.13
		Mantis	0.56 \pm 0.08	0.06 \pm 0.13	0.27 \pm 0.14
		MOMENT	0.51 \pm 0.06	0.03 \pm 0.10	0.22 \pm 0.12
		Chronos	0.56 \pm 0.09	0.07 \pm 0.14	0.28 \pm 0.10
		UME	0.58 \pm 0.09	0.03 \pm 0.13	0.26 \pm 0.12
WESAD	Low/High Valence	Dummy	0.51 \pm 0.06	0.07 \pm 0.07	0.80 \pm 0.10
		Gen. HC	0.55 \pm 0.15	0.01 \pm 0.17	0.66 \pm 0.18
		EDA-spec. HC	0.58 \pm 0.13	0.10 \pm 0.13	0.72 \pm 0.17
		Mantis	0.55 \pm 0.13	0.07 \pm 0.16	0.76 \pm 0.16
		MOMENT	0.63 \pm 0.07	0.03 \pm 0.07	0.76 \pm 0.14
		Chronos	0.56 \pm 0.10	0.05 \pm 0.11	0.77 \pm 0.15
		UME	0.59 \pm 0.13	0.08 \pm 0.12	0.77 \pm 0.13
APSYNC	Low/High engagement	Dummy	0.46 \pm 0.06	-0.09 \pm 0.11	0.29 \pm 0.16
		Gen. HC	0.61 \pm 0.13	0.14 \pm 0.25	0.53 \pm 0.26
		EDA-spec. HC	0.63 \pm 0.16	0.18 \pm 0.31	0.52 \pm 0.27
		Mantis	0.62 \pm 0.11	0.30 \pm 0.19	0.48 \pm 0.29
		MOMENT	0.60 \pm 0.20	0.24 \pm 0.39	0.61 \pm 0.21
		Chronos	0.48 \pm 0.16	-0.02 \pm 0.31	0.43 \pm 0.25
		UME	0.54 \pm 0.13	0.10 \pm 0.29	0.49 \pm 0.30
USILaughS	Cog. load/relax	Dummy	0.50 \pm 0.00	0.00 \pm 0.00	0.80 \pm 0.00
		Gen. HC	0.66 \pm 0.06	0.32 \pm 0.13	0.72 \pm 0.04
		EDA-spec. HC	0.70 \pm 0.09	0.40 \pm 0.19	0.70 \pm 0.11
		Mantis	0.72 \pm 0.09	0.43 \pm 0.19	0.76 \pm 0.10
		MOMENT	0.60 \pm 0.09	0.20 \pm 0.18	0.61 \pm 0.11
		Chronos	0.68 \pm 0.07	0.35 \pm 0.14	0.57 \pm 0.12
UME	0.71 \pm 0.11	0.42 \pm 0.22	0.76 \pm 0.10		

Table C.3: Results of binary classification experiments for Time-Aware (TA) cross-validation. Results shown as **metric \pm standard error**. Experiments whose result is reported as OoM (out of memory) means that the required memory size for the embeddings computation exceeded the computational resources available.

Dataset	Binary Task	Model	Metrics		
			Balanced Acc.	MCC	F1
Dreamt	Deep Sleep/REM	Dummy	0.51 \pm 0.01	0.01 \pm 0.01	0.20 \pm 0.06
		Gen. HC	0.55 \pm 0.10	0.09 \pm 0.20	0.28 \pm 0.13
		EDA-spec. HC	0.59 \pm 0.08	0.16 \pm 0.13	0.37 \pm 0.13
		Mantis	0.64 \pm 0.07	0.22 \pm 0.11	0.40 \pm 0.12
		MOMENT	0.65 \pm 0.04	0.24 \pm 0.07	0.42 \pm 0.10
		Chronos	0.64 \pm 0.04	0.23 \pm 0.08	0.41 \pm 0.10
		UME	0.63 \pm 0.09	0.20 \pm 0.13	0.38 \pm 0.11
Dreamt	Sleep/Wake	Dummy	0.50 \pm 0.01	-0.01 \pm 0.01	0.58 \pm 0.04
		Gen. HC	0.65 \pm 0.04	0.32 \pm 0.11	0.69 \pm 0.06
		EDA-spec. HC	0.69 \pm 0.01	0.38 \pm 0.03	0.72 \pm 0.02
		Mantis	0.73 \pm 0.02	0.46 \pm 0.03	0.76 \pm 0.02
		MOMENT	0.69 \pm 0.01	0.39 \pm 0.02	0.72 \pm 0.01
		Chronos	0.73 \pm 0.01	0.47 \pm 0.02	0.76 \pm 0.01
		UME	0.70 \pm 0.02	0.41 \pm 0.03	0.74 \pm 0.02
HHISS	Stress/calm	Dummy	0.50 \pm 0.00	-0.00 \pm 0.00	0.23 \pm 0.09
		Gen. HC	0.45 \pm 0.04	-0.10 \pm 0.07	0.34 \pm 0.04
		EDA-spec. HC	0.55 \pm 0.05	0.09 \pm 0.11	0.45 \pm 0.07
		Mantis	0.51 \pm 0.02	0.20 \pm 0.03	0.50 \pm 0.03
		MOMENT	OoM	OoM	OoM
		Chronos	OoM	OoM	OoM
		UME	0.49 \pm 0.06	-0.02 \pm 0.12	0.38 \pm 0.07
HeartS	Sleep/Wake	Dummy	0.49 \pm 0.00	-0.01 \pm 0.01	0.08 \pm 0.02
		Gen. HC	0.71 \pm 0.06	0.35 \pm 0.11	0.39 \pm 0.08
		EDA-spec. HC	0.72 \pm 0.14	0.36 \pm 0.25	0.41 \pm 0.20
		Mantis	0.75 \pm 0.16	0.40 \pm 0.28	0.45 \pm 0.23
		MOMENT	0.69 \pm 0.12	0.24 \pm 0.16	0.31 \pm 0.12
		Chronos	0.74 \pm 0.13	0.35 \pm 0.21	0.40 \pm 0.19
		UME	0.73 \pm 0.17	0.32 \pm 0.25	0.38 \pm 0.18
WESAD	Low/High Arousal	Dummy	0.55 \pm 0.05	0.08 \pm 0.07	0.15 \pm 0.07
		Gen. HC	0.56 \pm 0.15	0.08 \pm 0.22	0.26 \pm 0.11
		EDA-spec. HC	0.59 \pm 0.20	0.08 \pm 0.31	0.32 \pm 0.14
		Mantis	0.58 \pm 0.11	0.13 \pm 0.19	0.32 \pm 0.13
		MOMENT	OoM	OoM	OoM
		Chronos	0.56 \pm 0.18	0.07 \pm 0.28	0.28 \pm 0.20
		UME	0.56 \pm 0.12	0.08 \pm 0.18	0.28 \pm 0.15
WESAD	Low/High Valence	Dummy	0.51 \pm 0.03	0.01 \pm 0.04	0.66 \pm 0.06
		Gen. HC	0.54 \pm 0.20	0.08 \pm 0.33	0.76 \pm 0.12
		EDA-spec. HC	0.54 \pm 0.19	0.04 \pm 0.30	0.62 \pm 0.22
		Mantis	0.61 \pm 0.08	0.18 \pm 0.13	0.71 \pm 0.13
		MOMENT	OoM	OoM	OoM
		Chronos	0.45 \pm 0.12	-0.10 \pm 0.20	0.59 \pm 0.21
		UME	0.63 \pm 0.13	0.18 \pm 0.18	0.73 \pm 0.13
APSYNC	Low/High engagement	Dummy	0.45 \pm 0.20	0.13 \pm 0.13	0.13 \pm 0.13
		Gen. HC	0.81 \pm 0.20	0.32 \pm 0.32	0.72 \pm 0.29
		EDA-spec. HC	0.81 \pm 0.20	0.32 \pm 0.32	0.72 \pm 0.29
		Mantis	0.86 \pm 0.15	0.41 \pm 0.43	0.82 \pm 0.19
		MOMENT	0.48 \pm 0.32	-0.05 \pm 0.10	0.33 \pm 0.30
		Chronos	0.61 \pm 0.40	0.18 \pm 0.86	0.70 \pm 0.32
		UME	0.89 \pm 0.22	0.49 \pm 0.57	0.83 \pm 0.33